Simultaneous explanation of the R_K and $R_{D^{(*)}}$ puzzles: a model analysis

Bhubanjyoti Bhattacharya,[a,b] **Alakabha Datta,**[c,d] **Jean-Pascal Guévin,**[a] **David London**[a] **and Ryoutaro Watanabe**[a,e]

[a]*Physique des Particules, Université de Montréal,*
C.P. 6128, succ. centre-ville, Montréal, QC, H3C 3J7 Canada

[b]*Department of Physics and Astronomy, Wayne State University,*
Detroit, MI 48201, U.S.A.

[c]*Department of Physics and Astronomy, University of Mississippi,*
108 Lewis Hall, Oxford, MS 38677-1848, U.S.A.

[d]*Department of Physics and Astronomy,*
2505 Correa Rd, University of Hawaii, Honolulu, Hi 96826, U.S.A.

[e]*Center for Theoretical Physics of the Universe, Institute for Basic Science (IBS),*
Daejeon 305-811, Republic of Korea

E-mail: bhujyo@wayne.edu, datta@phy.olemiss.edu,
jean-pascal.guevin@umontreal.ca, london@lps.umontreal.ca,
watanabe@lps.umontreal.ca

ABSTRACT: R_K and $R_{D^{(*)}}$ are two B-decay measurements that presently exhibit discrepancies with the SM. Recently, using an effective field theory approach, it was demonstrated that a new-physics model can simultaneously explain both the R_K and $R_{D^{(*)}}$ puzzles. There are two UV completions that can give rise to the effective Lagrangian: (i) VB: a vector boson that transforms as an $SU(2)_L$ triplet, as in the SM, (ii) U_1: an $SU(2)_L$-singlet vector leptoquark. In this paper, we examine these models individually. A key point is that VB contributes to B_s^0-$\bar{B}_s^0$ mixing and $\tau \to 3\mu$, while U_1 does not. We show that, when constraints from these processes are taken into account, the VB model is just barely viable. It predicts $\mathcal{B}(\tau^- \to \mu^- \mu^+ \mu^-) \simeq 2.1 \times 10^{-8}$. This is measurable at Belle II and LHCb, and therefore constitutes a smoking-gun signal of VB. For U_1, there are several observables that may point to this model. Perhaps the most interesting is the lepton-flavor-violating decay $\Upsilon(3S) \to \mu\tau$, which has previously been overlooked in the literature. U_1 predicts $\mathcal{B}(\Upsilon(3S) \to \mu\tau)|_{\max} = 8.0 \times 10^{-7}$. Thus, if a large value of $\mathcal{B}(\Upsilon(3S) \to \mu\tau)$ is observed — and this should be measurable at Belle II — the U_1 model would be indicated.

Contents

1 Introduction

At present, there are several measurements of B decays that may indicate the presence of physics beyond the standard model (SM):

1. $b \to s\mu^+\mu^-$: the LHCb Collaboration has made measurements of $B \to K^*\mu^+\mu^-$ [1, 2] that deviate from the SM predictions [3]. The Belle Collaboration finds similar results [4]. The main discrepancy is in the angular observable P_5' [5]. The significance of the discrepancy depends on the assumptions about the theoretical hadronic uncertainties [6–8]. Indeed, it has been recently argued [9] that, by including non-factorizable power corrections, the experimental results can be reproduced within the SM. However, the latest fits to the data [10, 11], which take into account the hadronic uncertainties, find that a discrepancy is still present. It may reach the 4σ level.

   The LHCb Collaboration has also measured the branching fraction and performed an angular analysis of $B_s^0 \to \phi\mu^+\mu^-$ [12, 13]. They find a 3.5σ disagreement with the predictions of the SM, which are based on lattice QCD [14, 15] and QCD sum rules [16].

2. R_K: the LHCb Collaboration has found a hint of lepton non-universality. They measured the ratio $R_K \equiv \mathcal{B}(B^+ \to K^+\mu^+\mu^-)/\mathcal{B}(B^+ \to K^+e^+e^-)$ in the dilepton invariant mass-squared range $1\,\mathrm{GeV}^2 \le q^2 \le 6\,\mathrm{GeV}^2$ [17], and found

$$R_K^{\mathrm{expt}} = 0.745^{+0.090}_{-0.074}\ (\mathrm{stat}) \pm 0.036\ (\mathrm{syst})\,. \tag{1.1}$$

   This differs from the SM prediction of $R_K^{\mathrm{SM}} = 1 \pm 0.01$ [18] by 2.6σ, and is referred to as the R_K puzzle.

3. $R_{D^{(*)}}$: the charged-current decays $\bar{B} \to D^{(*)}\ell^-\bar{\nu}_\ell$ have been measured by the BaBar [19], Belle [20] and LHCb [21] Collaborations. It is found that the values of the ratios $R_{D^{(*)}} \equiv \mathcal{B}(\bar{B} \to D^{(*)}\tau^-\bar{\nu}_\tau)/\mathcal{B}(\bar{B} \to D^{(*)}\ell^-\bar{\nu}_\ell)$ $(\ell = e, \mu)$ considerably exceed their SM predictions. Assuming Gaussian distributions, and taking correlations into account, the experimental results and theoretical predictions can be combined to yield [22, 23]

$$R_D^{\mathrm{ratio}} \equiv \frac{R_D^{\mathrm{expt}}}{R_D^{\mathrm{SM}}} = 1.29 \pm 0.17\ , \quad R_{D^*}^{\mathrm{ratio}} \equiv \frac{R_{D^*}^{\mathrm{expt}}}{R_{D^*}^{\mathrm{SM}}} = 1.28 \pm 0.09\,. \tag{1.2}$$

   The measured values of R_D and R_{D^*} represent deviations from the SM of 1.7σ and 3.1σ, respectively. These are known as the R_D and R_{D^*} puzzles.

It must be stressed that, while the discrepancies in point 1 have some amount of theoretical input, those in points 2 and 3 are quite clean. As such, the R_K and $R_{D^{(*)}}$ puzzles provide very intriguing hints of new physics (NP).[1]

---

[1]Note that, while the R_K and $R_{D^{(*)}}$ puzzles require lepton-non-universal NP, this is not necessarily true for point 1, see ref. [24] for example.

In ref. [25], Hiller and Schmaltz searched for a NP explanation of the R_K puzzle. They performed a model-independent analysis of $b \to s\ell^+\ell^-$, considering NP operators of the form $(\bar{s}\mathcal{O}b)(\bar{\ell}\mathcal{O}'\ell)$, where $\mathcal{O}$ and $\mathcal{O}'$ span all Lorentz structures. They found that the only NP operator that can reproduce the experimental value of R_K is of $(V-A) \times (V-A)$ form: $(\bar{s}_L\gamma_\mu b_L)(\bar{\ell}_L\gamma^\mu\ell_L)$. Subsequent fits [26–28], which included both the $B \to K^*\mu^+\mu^-$ and R_K data, confirmed that such a NP operator can also account for the P'_5 discrepancy. To be specific, $b \to s\mu^+\mu^-$ transitions are defined via the effective Hamiltonian

$$H_{\text{eff}} = -\frac{\alpha G_F}{\sqrt{2}\pi}V_{tb}V_{ts}^* \sum_{a=9,10} \left(C_a O_a + C'_a O'_a\right),$$
$$O_{9(10)} = [\bar{s}_L\gamma_\mu b_L][\bar{\mu}\gamma^\mu(\gamma_5)\mu], \tag{1.3}$$

where the primed operators are obtained by replacing L with R. The Wilson coefficients $C_a^{(\prime)}$ include both SM and NP contributions. In the fits it was shown that a NP contribution to $b \to s\mu^+\mu^-$ is required; one of the possible solutions is $C_9^{\text{NP}} = -C_{10}^{\text{NP}} < 0$, with C_9^{NP} large. This corresponds to the $(\bar{s}_L\gamma_\mu b_L)(\bar{\ell}_L\gamma^\mu\ell_L)$ operator of ref. [25].

In ref. [29], Glashow, Guadagnoli and Lane (GGL) stressed that the NP responsible for lepton flavor non-universality will generally also lead to lepton-flavor-violating (LFV) effects. To illustrate this, they proposed the following explanation of the R_K puzzle. The NP is assumed to couple preferentially to the third generation with $(V-A) \times (V-A)$ form, giving rise to the operator

$$\frac{G}{\Lambda_{\text{NP}}^2}\left(\bar{b}'_L\gamma_\mu b'_L\right)\left(\bar{\tau}'_L\gamma^\mu\tau'_L\right), \tag{1.4}$$

where $G = O(1)$, $G/\Lambda_{\text{NP}}^2 \ll G_F$, and the primed fields are the fermion eigenstates in the gauge basis. When one transforms to the mass basis, this generates the operator $(\bar{b}_L\gamma_\mu s_L)(\bar{\mu}_L\gamma^\mu\mu_L)$ that contributes to $\bar{b} \to \bar{s}\mu^+\mu^-$. The contribution to $\bar{b} \to \bar{s}e^+e^-$ is much smaller, leading to a violation of lepton flavor universality. GGL's point was that LFV decays, such as $B \to K\mu e$, $K\mu\tau$ and $B_s^0 \to \mu e, \mu\tau$, are also generated.

In ref. [30], it was pointed out that, assuming the scale of NP is much larger than the weak scale, the operator of eq. (1.4) should be made invariant under the full $\text{SU}(3)_C \times \text{SU}(2)_L \times \text{U}(1)_Y$ gauge group. There are two possibilities:

$$\mathcal{O}_1^{\text{NP}} = \frac{G_1}{\Lambda_{\text{NP}}^2}\left(\bar{Q}'_L\gamma_\mu Q'_L\right)\left(\bar{L}'_L\gamma^\mu L'_L\right),$$
$$\mathcal{O}_2^{\text{NP}} = \frac{G_2}{\Lambda_{\text{NP}}^2}\left(\bar{Q}'_L\gamma_\mu\sigma^I Q'_L\right)\left(\bar{L}'_L\gamma^\mu\sigma^I L'_L\right)$$
$$= \frac{G_2}{\Lambda_{\text{NP}}^2}\left[2\left(\bar{Q}'^i_L\gamma_\mu Q'^j_L\right)\left(\bar{L}'^j_L\gamma^\mu L'^i_L\right) - \left(\bar{Q}'_L\gamma_\mu Q'_L\right)\left(\bar{L}'_L\gamma^\mu L'_L\right)\right], \tag{1.5}$$

where G_1 and G_2 are both $O(1)$, and the σ^I are the Pauli matrices. Here $Q' \equiv (t', b')^T$ and $L' \equiv (\nu'_\tau, \tau')^T$. The key point is that $\mathcal{O}_2^{\text{NP}}$ contains both neutral-current (NC) and charged-current (CC) interactions. The NC and CC pieces can be used to respectively

explain the R_K and $R_{D^{(*)}}$ puzzles.[2] (Of course, while a common model of these anomalies is intriguing, it is also more constraining than separate explanations of the two puzzles.)

This method was explored in greater detail in ref. [44]. The starting point is the model-independent effective Lagrangian based on eq. (1.5):

$$\mathcal{L}_{\mathrm{NP}} = \frac{G_1}{\Lambda_{\mathrm{NP}}^2} \left(\bar{Q}'_L \gamma_\mu Q'_L \right) \left(\bar{L}'_L \gamma^\mu L'_L \right) + \frac{G_2}{\Lambda_{\mathrm{NP}}^2} \left(\bar{Q}'_L \gamma_\mu \sigma^I Q'_L \right) \left(\bar{L}'_L \gamma^\mu \sigma^I L'_L \right). \qquad (1.6)$$

These operators are written in the gauge basis and involve only third-generation fermions. In transforming from the gauge basis to the mass basis, the left-handed down- and up-type quarks are operated upon by the matrices D and U, respectively, where the Cabibbo-Kobayashi-Maskawa (CKM) matrix is $V_{CKM} = U^\dagger D$. The leptons are different: neglecting the neutrino masses, the left-handed charged and neutral leptons are both operated upon by the same matrix L. In ref. [44] it is assumed that the transformations D and L lead to mixing only between the second and third generations, so that they each depend on only one unknown theoretical parameter, respectively θ_D and θ_L. In the mass basis, the above operators contribute to a variety of B decays. Ref. [44] considers the following processes/observables: (i) $b \to s \ell^+ \ell^-$ ($\ell = \mu, e$): $B \to K^* \mu^+ \mu^-$, $B_s^0 \to \phi \mu^+ \mu^-$, R_K, (ii) $b \to c \tau^- \bar{\nu}_\tau$: $R_{D^{(*)}}$, (iii) $b \to s \nu \bar{\nu}$: $B \to K^{(*)} \nu \bar{\nu}$ [45, 46]. The experimental measurements thus put constraints on the coefficients, which are all functions of G_1, G_2, θ_D and θ_L. When all constraints are taken into account, it is found that the R_K and $R_{D^{(*)}}$ puzzles can be simultaneously explained if θ_L is of the order of $\pi/16$ and θ_D is very small (less than V_{cb}). With these values for θ_L and θ_D, one can make predictions for the rates of other (LFV) processes, and this is done for $B \to K^{(*)} \ell \ell'$ and $B_s^0 \to \ell \ell'$ ($\ell \ell' = \tau \mu, \tau e, \mu e$).

Finally, ref. [44] considers possible UV completions that can give rise to $\mathcal{O}_2^{\mathrm{NP}}$ [eq. (1.5)], that is required to explain both R_K and $R_{D^{(*)}}$. Its coefficient $(G_2/\Lambda_{\mathrm{NP}}^2)$ suggests that this operator is generated by the tree-level exchange of a single particle. In this case, there are only four possibilities for the underlying NP model: (i) a vector boson (VB) that transforms as $(\mathbf{1}, \mathbf{3}, 0)$ under $\mathrm{SU}(3)_C \times \mathrm{SU}(2)_L \times \mathrm{U}(1)_Y$, as in the SM, (ii) an $\mathrm{SU}(2)_L$-triplet scalar leptoquark (S_3) $[(\mathbf{3}, \mathbf{3}, -2/3)]$, (iii) an $\mathrm{SU}(2)_L$-singlet vector leptoquark (U_1) $[(\mathbf{3}, \mathbf{1}, 4/3)]$, (iv) an $\mathrm{SU}(2)_L$-triplet vector leptoquark (U_3) $[(\mathbf{3}, \mathbf{3}, 4/3)]$. The vector boson generates only $\mathcal{O}_2^{\mathrm{NP}}$, but the leptoquarks generate particular combinations of $\mathcal{O}_1^{\mathrm{NP}}$ and $\mathcal{O}_2^{\mathrm{NP}}$ [47]. It is shown that the combination of $\mathcal{O}_1^{\mathrm{NP}}$ and $\mathcal{O}_2^{\mathrm{NP}}$ generated by the S_3 and U_3 leptoquarks cannot simultaneously explain R_K and $R_{D^{(*)}}$. The only possible UV completions are therefore the VB and U_1 models.

But this now raises a question. If the NP responsible for the R_K and $R_{D^{(*)}}$ puzzles leads to the effective Lagrangian of eq. (1.6), the underlying NP model is either VB or U_1. But which is it? Short of actually producing a W'/Z' or a leptoquark in an experiment, is there any way of distinguishing the two models? At first glance, the answer is no. After all, the two models lead to the same effective Lagrangian and so are "equivalent." However, this is not really true. To see this, one has to understand the difference between analyses

---

[2]Other analyses of the $R_{D^{(*)}}$ puzzle can be found in refs. [31–37]. Distributions in $\bar{B} \to D^{(*)} \tau^- \bar{\nu}_\tau$ decays can provide information on the type of new physics present in these decays [38–40]. Efforts to simultaneously explain multiple flavor anomalies can be found in refs. [41–43].

based on an effective field theory (EFT) and those based on models. In an EFT analysis, one writes all effective operators of a given order; these are considered as independent. The effective Lagrangian of eq. (1.6) includes all four-fermion operators containing two quarks and two leptons. One can also write four-quark and four-lepton operators. But since these are uncorrelated with the operators with two quarks and two leptons, and since only processes of the type $q \to q'\ell\ell^{(\prime)}$ are studied, these other operators are uninteresting. But this does not hold in a model analysis. Concretely, while both VB and U_1 models lead to operators with two quarks and two leptons, VB also produces four-quark and four-lepton operators at tree level. In particular, it will contribute significantly to B_s^0-$\bar{B}_s^0$ mixing and the lepton-flavor-violating decay $\tau \to 3\mu$. These will lead to additional constraints on θ_D and θ_L, respectively. Furthermore, while VB contributes to $B \to K^{(*)}\nu\bar{\nu}$, U_1 does not. The bottom line is that the experimental constraints on the VB model are more stringent than those on the U_1 model. Thus, the predictions for the rates of other processes can be very different in the two models, and this may allow us to distinguish them. It is this feature that is studied in the present paper.

We begin in section 2 by reviewing the method of ref. [44] for generating contributions to R_K and $R_{D^{(*)}}$, as well as the NP models in which this can occur. These include the vector-boson model VB and the S_3, U_1 and U_3 leptoquark models. The experimental measurements that constrain these models are described in section 3. These include not only processes involving $b \to s\ell^+\ell^-$, $b \to s\nu\bar{\nu}$ and $b \to c\tau^-\bar{\nu}$, but also $\tau \to \mu\phi$, B_s^0-$\bar{B}_s^0$ mixing and $\tau \to 3\mu$. These experimental constraints are applied to the models in section 4. As in ref. [44], we find that S_3 and U_3 are excluded, leaving only VB and U_1. However, the constraints from B_s^0-$\bar{B}_s^0$ mixing and $\tau \to 3\mu$ are so stringent that the VB model is only barely viable. In section 5 we examine the predictions of VB and U_1 for other processes, to see if the two models can be distinguished. We find that, in fact, there are a number of different ways of doing this. Useful processes/observables include $\tau \to 3\mu$, R_K, and a previously overlooked lepton-flavor-violating decay, $\Upsilon \to \mu\tau$. We conclude in section 6.

2 Models

Including the generation indices i, j, k, l, the effective Lagrangian of eq. (1.6) can be written as

$$\mathcal{L}_{\rm NP} = \frac{G_1^{ijkl}}{\Lambda_{\rm NP}^2} \left(\bar{Q}_L^{(\prime)i} \gamma_\mu Q_L^{(\prime)j} \right) \left(\bar{L}_L^{(\prime)k} \gamma^\mu L_L^{(\prime)l} \right) + \frac{G_2^{ijkl}}{\Lambda_{\rm NP}^2} \left(\bar{Q}_L^{(\prime)i} \gamma_\mu \sigma^I Q_L^{(\prime)j} \right) \left(\bar{L}_L^{(\prime)k} \gamma^\mu \sigma^I L_L^{(\prime)l} \right).$$
(2.1)

This holds in both the gauge and mass bases. The gauge eigenstates, which involve only third-generation fermions, are indicated by primes on the spinors; the mass eigenstates have no primes. In transforming from the gauge basis to the mass basis, we have

$$u_L' = U u_L, \quad d_L' = D d_L, \quad \ell_L' = L \ell_L, \quad \nu_L' = L \nu_L,$$
(2.2)

where U, D and L are 3×3 unitary matrices and the spinors $u^{(\prime)}$, $d^{(\prime)}$, $\ell^{(\prime)}$ and $\nu^{(\prime)}$ include all three generations of fermions. The fact that the left-handed charged and neutral leptons are

both operated upon by the same matrix L is a result of neglecting the neutrino masses.[3] The CKM matrix is given by $V_{CKM} = U^\dagger D$. The assumption of ref. [44] is that the transformations D and L involve only the second and third generations:

$$D = \begin{pmatrix} 1 & 0 & 0 \\ 0 & \cos\theta_D & \sin\theta_D \\ 0 & -\sin\theta_D & \cos\theta_D \end{pmatrix} \;, \qquad L = \begin{pmatrix} 1 & 0 & 0 \\ 0 & \cos\theta_L & \sin\theta_L \\ 0 & -\sin\theta_L & \cos\theta_L \end{pmatrix}. \tag{2.3}$$

Because of these transformations, for the down-type quarks and charged leptons, couplings involving the second generation (possibly flavor-changing) are possible in the mass basis. (For the up-type quarks, the first generation can also be involved.)

Specifically, in the mass basis we have

$$G_n^{ijkl} = g_n X^{ij} Y^{kl} \,, \tag{2.4}$$

where X and Y include the transformations from the gauge to the mass basis. The exact forms of these matrices depend on which four-fermion operator is used. For the decay $b \to s\ell^+\ell^-$ we have

$$X = D^\dagger \begin{pmatrix} 0\ 0\ 0 \\ 0\ 0\ 0 \\ 0\ 0\ 1 \end{pmatrix} D = \begin{pmatrix} 0 & 0 & 0 \\ 0 & \sin^2\theta_D & -\sin\theta_D\cos\theta_D \\ 0 & -\sin\theta_D\cos\theta_D & \cos^2\theta_D \end{pmatrix} \,,$$

$$Y = L^\dagger \begin{pmatrix} 0\ 0\ 0 \\ 0\ 0\ 0 \\ 0\ 0\ 1 \end{pmatrix} L = \begin{pmatrix} 0 & 0 & 0 \\ 0 & \sin^2\theta_L & -\sin\theta_L\cos\theta_L \\ 0 & -\sin\theta_L\cos\theta_L & \cos^2\theta_L \end{pmatrix}. \tag{2.5}$$

If up-type quarks are involved in a process (such as $b \to c\tau^-\bar\nu$), one must include the transformation matrix U [eq. (2.2)]. Because $V_{CKM} = U^\dagger D$, the amplitude will involve factors of V_{CKM} in addition to X and Y.

In terms of components, the effective Lagrangian is

$$\mathcal{L}_{\text{NP}} = \frac{\left(G_1^{ijkl} + G_2^{ijkl}\right)}{\Lambda_{\text{NP}}^2} \left[\left(\bar{u}_L^i \gamma_\mu u_L^j\right)\left(\bar{\nu}_L^k \gamma^\mu \nu_L^l\right) + \left(\bar{d}_L^i \gamma_\mu d_L^j\right)\left(\bar{\ell}_L^k \gamma^\mu \ell_L^l\right) \right]$$

$$+ \frac{\left(G_1^{ijkl} - G_2^{ijkl}\right)}{\Lambda_{\text{NP}}^2} \left[\left(\bar{u}_L^i \gamma_\mu u_L^j\right)\left(\bar{\ell}_L^k \gamma^\mu \ell_L^l\right) + \left(\bar{d}_L^i \gamma_\mu d_L^j\right)\left(\bar{\nu}_L^k \gamma^\mu \nu_L^l\right) \right]$$

$$+ 2\, \frac{G_2^{ijkl}}{\Lambda_{\text{NP}}^2} \left[\left(\bar{u}_L^i \gamma_\mu d_L^j\right)\left(\bar{\ell}_L^k \gamma^\mu \nu_L^l\right) + \text{h.c.} \right]. \tag{2.6}$$

---

[3]If neutrino masses are not neglected, the matrices L and N operate on the left-handed charged and neutral leptons, respectively, and the Pontecorvo-Maki-Nakagawa-Sakata (PMNS) matrix is $V_{PMNS} = N^\dagger L$. However, in processes such as $b \to c\tau^-\bar\nu_\tau$ and $b \to s\nu\bar\nu$, the final-state neutrinos are not detected, and so one must sum over all neutrinos. In this case, since V_{PMNS} is unitary ($V_{PMNS}^\dagger V_{PMNS} = 1$), its effect on these processes vanishes.

For the processes of interest, the NP contributions are

$$b \to s\mu^+\mu^- \;:\; \frac{(g_1 + g_2)}{\Lambda^2_{\rm NP}} X^{23} Y^{22} \left(\bar{s}_L \gamma_\mu b_L\right)\left(\bar{\mu}_L \gamma^\mu \mu_L\right) + \text{h.c.}\,, \tag{2.7}$$

$$b \to s\nu\bar{\nu} \;:\; \frac{(g_1 - g_2)}{\Lambda^2_{\rm NP}} X^{23} Y^{kl} \left(\bar{s}_L \gamma_\mu b_L\right)\left(\bar{\nu}^k_L \gamma^\mu \nu^l_L\right) + \text{h.c.} \quad \text{for } k,l = 2,3\,, \tag{2.8}$$

$$b \to c\tau^-\bar{\nu} \;:\; \frac{2g_2}{\Lambda^2_{\rm NP}} \left[(V_{CKM} X)^{23} Y^{3l} \left(\bar{c}_L \gamma_\mu b_L\right)\left(\bar{\tau}_L \gamma^\mu \nu^l_L\right) + \text{h.c.} \right] \quad \text{for } l = 2,3\,. \tag{2.9}$$

From these expressions, we see that there is no NP contribution to $b \to s\nu\bar{\nu}$ ($b \to s\mu^+\mu^-$) if $g_1 = g_2$ ($g_1 = -g_2$).

In the above, the NP is described in effective field theory language, as in ref. [44]. However, we are interested in explicitly studying the models that can lead to this EFT. There are two categories of NP models, those with new vector bosons, and those that involve leptoquarks. Below we summarize the features of the various models.

2.1 SM-like vector bosons

This model contains vector bosons (VBs) that transform as $(\mathbf{1}, \mathbf{3}, 0)$ under $\text{SU}(3)_C \times \text{SU}(2)_L \times \text{U}(1)_Y$, as in the SM. We refer to the VBs as $V = W'$, Z'.

In the gauge basis, the Lagrangian describing the couplings of the VBs to left-handed third-generation fermions is

$$\Delta\mathcal{L}_V = g^{33}_{qV} \left(\overline{Q}'_{L3}\,\gamma^\mu \sigma^I\, Q'_{L3}\right) V^I_\mu \;+\; g^{33}_{\ell V} \left(\overline{L}'_{L3}\,\gamma^\mu \sigma^I\, L'_{L3}\right) V^I_\mu\,, \tag{2.10}$$

where σ^I ($I = 1,2,3$) are the Pauli matrices. Once the heavy VB is integrated out, we obtain the following effective Lagrangian, relevant for $b \to s\ell^+\ell^-$, $b \to c\tau^-\bar{\nu}$ and $b \to s\nu\bar{\nu}$ decays:

$$\mathcal{L}^{\rm eff}_V = -\frac{g^{33}_{qV} g^{33}_{\ell V}}{m^2_V} \left(\overline{Q}'_{L3}\gamma^\mu \sigma^I\, Q'_{L3}\right)\left(\overline{L}'_{L3}\gamma_\mu \sigma^I L'_{L3}\right)\,. \tag{2.11}$$

Comparing this with eq. (2.1), we find

$$g_1 = 0 \;,\quad g_2 = -g^{33}_{qV} g^{33}_{\ell V}\,. \tag{2.12}$$

Note that g_2 can be either positive or negative in this model.

When one transforms to the mass basis, the VBs couple to other generations. The Z' contributes at tree level to $b \to s\mu^+\mu^-$ and $b \to s\nu\bar{\nu}$; the W' contributes at tree level to $b \to c\tau^-\bar{\nu}$. These contributions are given in eqs. (2.7)–(2.9) for the above values of g_1 and g_2.

The above processes all involve four-fermion operators that contain two quarks and two leptons. But VB exchange also produces four-quark and four-lepton operators at tree level. In the gauge basis, the corresponding effective Lagrangian is

$$\begin{aligned}\mathcal{L}^{4Q,4L}_{\rm NP} = {} & -\frac{\left(g^{33}_{qV}\right)^2}{2m^2_V} \left(\overline{Q}'_{L3}\gamma^\mu \sigma^I Q'_{L3}\right)\left(\overline{Q}'_{L3}\gamma_\mu \sigma^I Q'_{L3}\right) \\ & -\frac{\left(g^{33}_{\ell V}\right)^2}{2m^2_V} \left(\overline{L}'_{L3}\gamma^\mu \sigma^I L'_{L3}\right)\left(\overline{L}'_{L3}\gamma_\mu \sigma^I L'_{L3}\right)\,.\end{aligned} \tag{2.13}$$

Fierz Transformations
$(\overline{a}_L b_L^c)(\overline{c}_L^c d_L) = -\frac{1}{2}(\overline{a}_L \gamma^\mu d_L)(\overline{c}_L^c \gamma_\mu b_L^c)$
$(\overline{a}_L \gamma^\mu b_L)(\overline{c}_L \gamma_\mu d_L) = (\overline{a}_L \gamma^\mu d_L)(\overline{c}_L \gamma_\mu b_L)$
Identities involving Pauli Matrices
$\sigma_{ij}^2 \sigma_{kl}^2 = \frac{1}{2}\delta_{il}\delta_{kj} - \frac{1}{2}\sigma_{il}^I \cdot (\sigma^I)_{kj}^T$
$\sigma_{ij}^I \sigma_{jk}^2 \sigma_{lm}^2 \sigma_{mn}^I = \frac{3}{2}\delta_{in}\delta_{lk} + \frac{1}{2}\sigma_{in}^I \cdot (\sigma^I)_{lk}^T$
$\delta_{ij}\delta_{kl} = \frac{1}{2}\delta_{il}\delta_{kj} + \frac{1}{2}\sigma_{il}^I \cdot \sigma_{kj}^I$
$\sigma_{ij}^I \sigma_{kl}^I = \frac{3}{2}\delta_{il}\delta_{kj} - \frac{1}{2}\sigma_{il}^I \cdot \sigma_{kj}^I$

Table 1. Fierz transformations and Pauli-matrix identities used in the analysis of LQ models.

In the mass basis, these contribute to processes such as B_s^0-$\bar{B}_s^0$ mixing and $\tau \to 3\mu$, and their measurements can be used to further constrain the VB model.

There are a number of variants of the VB model — for example, see refs. [48–52]. Note that some of these models address the $b \to s\mu^+\mu^-$ anomalies with a Z', while others also try to explain the $R_{D^{(*)}}$ puzzle. In some models, new fermions are involved. This introduce additional parameters, which can lead to more flexibility in predictions.

2.2 Leptoquarks

In refs. [35, 53] it was shown that six different types of leptoquark (LQ) models can explain $R_{D^{(*)}}$. Of these, only four lead to four-fermion operators of the desired $(V - A) \times (V - A)$ form: (i) a scalar $SU(2)_L$ singlet S_1, (ii) a scalar $SU(2)_L$ triplet S_3, (iii) a vector $SU(2)_L$ singlet U_1, (iv) a vector $SU(2)_L$ triplet U_3. In general, tree-level LQ exchange generates $\mathcal{O}_1^{\mathrm{NP}}$ and $\mathcal{O}_2^{\mathrm{NP}}$ [47]. However, different models will produce different combinations of the two operators. Below, with the help of the identities in table 1, we determine these combinations for each of the four LQ models. That is, we derive the relation between g_1 and g_2, as well as the signs of these quantities.

Note that, unlike the VB model, four-quark and four-lepton operators are not produced in LQ models at tree level.

2.2.1 $SU(2)_L$-singlet scalar LQ (S_1)

S_1 is a scalar LQ that is an $SU(2)_L$ triplet (it transforms as $(\mathbf{3}, \mathbf{1}, -2/3)$ under $SU(3)_C \times SU(2)_L \times U(1)_Y$). In the gauge basis, the interaction Lagrangian for the S_1 LQ is given by [53]

$$\Delta\mathcal{L}_{S_1} = h_{S_1}^{33}\left(\overline{Q}'_{L3} i\sigma^2 L_{L3}'^c\right)S_1 + \text{h.c.}, \tag{2.14}$$

where $\psi^c = C\bar{\psi}^T$ denotes a charge-conjugated fermion field. When the heavy LQ is integrated out, we obtain the following effective Lagrangian:

$$\mathcal{L}_{S_1}^{\text{eff}} = \frac{\left|h_{S_1}^{33}\right|^2}{m_{S_1}^2} \left(\overline{Q}'_{L3i}\sigma_{ij}^2 L'^c_{L3j}\right) \left(\overline{L}'^c_{L3k}\sigma_{kl}^2 Q'_{L3l}\right) \tag{2.15}$$

$$= \frac{\left|h_{S_1}^{33}\right|^2}{4m_{S_1}^2} \left[\left(\overline{Q}'_{L3}\gamma^\mu Q'_{L3}\right) \left(\overline{L}'_{L3}\gamma_\mu L'_{L3}\right) - \left(\overline{Q}'_{L3}\gamma^\mu\sigma^I Q'_{L3}\right) \left(\overline{L}'_{L3}\gamma_\mu\sigma^I L'_{L3}\right)\right] .$$

$SU(2)_L$ indices have been inserted in the first line. In the second line, we have used relations from table 1 and then suppressed the indices. Comparing this with eq. (2.1), we find

$$g_1 = -g_2 = \frac{1}{4}\left|h_{S_1}^{33}\right|^2 > 0 . \tag{2.16}$$

When one transforms to the mass basis, the S_1 LQ couples to other generations. However, because $g_1 = -g_2$, it does not contribute to $b \to s\mu^+\mu^-$ [eq. (2.7)] and hence cannot explain R_K. So this LQ model is not of interest to us.

2.2.2 $SU(2)_L$-triplet scalar LQ (S_3)

S_3 is a scalar LQ that is an $SU(2)_L$ triplet (it transforms as $(\mathbf{3}, \mathbf{3}, -2/3)$). In the gauge basis, its interaction Lagrangian is given by [53]

$$\Delta\mathcal{L}_{S_3} = h_{S_3}^{33} \left(\overline{Q}'_{L3}\sigma^I i\sigma^2 L'^c_{L3}\right) S_3^I + \text{h.c.} \tag{2.17}$$

Integrating out the heavy LQ, we obtain the following effective Lagrangian:

$$\mathcal{L}_{S_3}^{\text{eff}} = \frac{\left|h_{S_3}^{33}\right|^2}{m_{S_3}^2} \left(\overline{Q}'_{L3i}\sigma_{ij}^I \sigma_{jk}^2 L'^c_{L3k}\right) \left(\overline{L}'^c_{L3l}\sigma_{lm}^2 \sigma_{mn}^I Q'_{L3n}\right) \tag{2.18}$$

$$= \frac{\left|h_{S_3}^{33}\right|^2}{4m_{S_3}^2} \left[3\left(\overline{Q}'_{L3}\gamma^\mu Q'_{L3}\right) \left(\overline{L}'_{L3}\gamma_\mu L'_{L3}\right) + \left(\overline{Q}'_{L3}\gamma^\mu\sigma^I Q'_{L3}\right) \left(\overline{L}'_{L3}\gamma_\mu\sigma^I L'_{L3}\right)\right] .$$

Comparing this with eq. (2.1), we find

$$g_1 = 3g_2 = \frac{3}{4}\left|h_{S_3}^{33}\right|^2 > 0 . \tag{2.19}$$

When one transforms to the mass basis, the S_3 LQ couples to other generations. The components of the $SU(2)_L$ triplet have $Q_{em} = \frac{2}{3}, -\frac{1}{3}, -\frac{4}{3}$. The $Q_{em} = \frac{2}{3}$ LQ contributes to $b \to s\ell^+\ell^-$ and $b \to c\tau^-\bar{\nu}$, while the $Q_{em} = -\frac{1}{3}$ LQ contributes to $b \to s\nu\bar{\nu}$. These contributions are given in eqs. (2.7)–(2.9) for the above values of g_1 and g_2.

The S_3 LQ has been studied in refs. [54, 55].

2.2.3 $SU(2)_L$-singlet vector LQ (U_1)

U_1 is a vector LQ that is an $SU(2)_L$ singlet (it transforms as $(\mathbf{3}, \mathbf{1}, 4/3)$). Its interaction Lagrangian is given in the gauge basis by [53]

$$\Delta\mathcal{L}_{U_1} = h_{U_1}^{33} \left(\overline{Q}'_{L3} \gamma^\mu L'_{L3}\right) U_{1\mu} + \text{h.c.} \tag{2.20}$$

Integrating out the heavy LQ, and inserting $SU(2)_L$ indices, we obtain the following effective Lagrangian:

$$\mathcal{L}_{U_1}^{\text{eff}} = -\frac{\left|h_{U_1}^{33}\right|^2}{m_{U_1}^2} \left(\overline{Q}_{L3i}' \gamma^\mu \delta_{ij} \, L_{L3j}'\right) \left(\overline{L}_{L3k}' \gamma_\mu \delta_{kl} \, Q_{L3l}'\right) \tag{2.21}$$

$$= -\frac{\left|h_{U_1}^{33}\right|^2}{2m_{U_1}^2} \left[\left(\overline{Q}_{L3}' \gamma^\mu Q_{L3}'\right) \left(\overline{L}_{L3}' \gamma^\mu L_{L3}'\right) + \left(\overline{Q}_{L3}' \gamma^\mu \sigma^I Q_{L3}'\right) \left(\overline{L}_{L3}' \gamma_\mu \sigma^I L_{L3}'\right)\right] .$$

Comparing this with eq. (2.1), we find

$$g_1 = g_2 = -\frac{1}{2}\left|h_{U_1}^{33}\right|^2 < 0 . \tag{2.22}$$

In the mass basis, the U_1 LQ couples to other generations and contributes at tree level to $b \to s\mu^+\mu^-$ and $b \to c\tau^-\bar{\nu}$. These contributions are given in eqs. (2.7) and (2.9) for the above values of g_1 and g_2. However, because $g_1 = g_2$, there is no contribution to $b \to s\nu\bar{\nu}$.

The U_1 LQ has been studied in ref. [56].

2.2.4 $SU(2)_L$-triplet vector LQ (U_3)

The U_3 LQ is a vector that is an $SU(2)_L$ triplet (it transforms as $(\mathbf{3}, \mathbf{3}, 4/3)$). In the gauge basis, its interaction Lagrangian is given by [53]

$$\Delta\mathcal{L}_{U_3} = h_{U_3}^{33} \left(\overline{Q}_{L3}' \, \gamma^\mu \, \sigma^I L_{L3}'\right) U_{3\mu}^I \; + \; \text{h.c.} \tag{2.23}$$

When the heavy LQ is integrated out, the effective Lagrangian is

$$\mathcal{L}_{U_3}^{\text{eff}} = -\frac{\left|h_{U_3}^{33}\right|^2}{m_{U_3}^2} \left(\overline{Q}_{L3i}' \gamma^\mu \sigma_{ij}^I \, L_{L3j}'\right) \left(\overline{L}_{L3k}' \gamma_\mu \sigma_{kl}^I \, Q_{L3l}'\right) \tag{2.24}$$

$$= -\frac{\left|h_{U_3}^{33}\right|^2}{2m_{U_3}^2} \left[3\left(\overline{Q}_{L3}' \gamma^\mu Q_{L3}'\right) \left(\overline{L}_{L3}' \gamma^\mu L_{L3}'\right) - \left(\overline{Q}_{L3}' \gamma^\mu \sigma^I Q_{L3}'\right) \left(\overline{L}_{L3}' \gamma_\mu \sigma^I L_{L3}'\right)\right] .$$

Comparing this with eq. (2.1), we find

$$g_1 = -3g_2 = -\frac{3}{2}\left|h_{U_3}^{33}\right|^2 < 0 . \tag{2.25}$$

In the mass basis, the U_3 LQ couples to other generations. The components of the $SU(2)_L$ triplet have $Q_{em} = \frac{5}{3}, \frac{2}{3}, -\frac{1}{3}$. The $Q_{em} = \frac{2}{3}$ LQ contributes to $b \to s\ell^+\ell^-$ and $b \to c\tau^-\bar{\nu}$; the $Q_{em} = -\frac{1}{3}$ LQ contributes to $b \to s\nu\bar{\nu}$. These contributions are given in eqs. (2.7)–(2.9) for the above values of g_1 and g_2.

The U_3 LQ has been studied in refs. [57, 58].

2.3 Summary

We briefly recap the above results. We assume that the NP couples only to the third generation in the gauge basis, and that it produces four-fermion operators with a $(V - A) \times (V - A)$ structure. We find that there are four NP models that contribute to both R_K

and $R_{D^{(*)}}$. There are two operators, $\mathcal{O}_1^{\text{NP}}$ and $\mathcal{O}_2^{\text{NP}}$, shown in eq. (2.1), whose coefficients are g_1 and g_2. The four models contribute differently to $\mathcal{O}_1^{\text{NP}}$ and $\mathcal{O}_2^{\text{NP}}$:

$$
\begin{aligned}
VB &: g_1 = 0 \,, \quad g_2 = -g_{qV}^{33} g_{\ell V}^{33} \,, \quad g_2 \text{ can be positive or negative} \,, \\
S_3 &: g_1 = 3g_2 = \frac{3}{4} \left| h_{S_3}^{33} \right|^2 > 0 \,, \\
U_1 &: g_1 = g_2 = -\frac{1}{2} \left| h_{U_1}^{33} \right|^2 < 0 \,, \\
U_3 &: g_1 = -3g_2 = -\frac{3}{2} \left| h_{U_3}^{33} \right|^2 < 0 \,.
\end{aligned}
\tag{2.26}
$$

In ref. [44], it is noted that $\lambda^{(3)} (= g_2)$ is positive for the S_3 and U_3 models, but negative for U_1. This is confirmed by the above.

3   Constraints

When one transforms to the mass basis, two new parameters are introduced, θ_D, θ_L. The NP contributes to $b \to s\mu^+\mu^-$, $b \to s\nu\bar{\nu}$ and $b \to c\tau^-\bar{\nu}$. These contributions are given in eqs. (2.7)–(2.9); the coefficients are (different) functions of g_1, g_2, θ_D, θ_L. Another decay to which all four models contribute is $\tau \to \mu\phi$. In addition, the VB model contributes to other processes, such as B_s^0-$\bar{B}_s^0$ mixing and $\tau \to 3\mu$. The experimental measurements of, or limits on, these processes provide constraints on the NP parameter space.

In order to compare models, we fix $\Lambda_{\text{NP}} = 1\,\text{TeV}$ and assume a common value for $2g_{qV}^{33} g_{\ell V}^{33}$, $\left| h_{S_3}^{33} \right|^2$, $\left| h_{U_1}^{33} \right|^2$ and $\left| h_{U_3}^{33} \right|^2$. We apply all the experimental constraints to establish the allowed region in the (θ_D, θ_L) parameter space. If there is no region in which all constraints overlap, the model is excluded. For the models that are retained, we predict the rates for other processes based on the allowed region in parameter space. Since this region can be different for different models, it may be possible to distinguish them.

3.1 $b \to s\ell^+\ell^-$, $b \to s\nu\bar{\nu}$, $b \to c\tau^-\bar{\nu}$

The effective Hamiltonians for $b \to s\ell^+\ell^-$, $b \to s\nu\bar{\nu}$ and $b \to c\tau^-\bar{\nu}$ are

$$
\begin{aligned}
H_{\text{eff}} \left(b \to s\ell_i \bar{\ell}_j \right) = -\frac{\alpha G_F}{\sqrt{2}\pi} V_{tb} V_{ts}^* \Big[& C_9^{ij} \left(\bar{s}_L \gamma^\mu b_L \right) \left(\bar{\ell}_i \gamma_\mu \ell_j \right) \\
& + C_{10}^{ij} \left(\bar{s}_L \gamma^\mu b_L \right) \left(\bar{\ell}_i \gamma_\mu \gamma^5 \ell_j \right) \Big] \,,
\end{aligned}
\tag{3.1}
$$

$$
H_{\text{eff}} \left(b \to s\nu_i \bar{\nu}_j \right) = -\frac{\alpha G_F}{\sqrt{2}\pi} V_{tb} V_{ts}^* C_L^{ij} \left(\bar{s}_L \gamma^\mu b_L \right) \left(\bar{\nu}_i \gamma_\mu (1 - \gamma^5) \nu_j \right) \,,
\tag{3.2}
$$

$$
H_{\text{eff}} \left(b \to c\ell_i \bar{\nu}_j \right) = \frac{4 G_F}{\sqrt{2}} V_{cb} C_V^{ij} \left(\bar{c}_L \gamma^\mu b_L \right) \left(\bar{\ell}_{iL} \gamma_\mu \nu_{jL} \right) \,,
\tag{3.3}
$$

where the Wilson coefficients include both the SM and NP contributions: $C_X = C_X(\text{SM}) + C_X(\text{NP})$. Comparing with eqs. (2.7)–(2.9) (and recalling that $\mathcal{L}_{\text{NP}}$ and H_{eff} have opposite

signs), we have

$$C_9^{ij}(\text{NP}) = -C_{10}^{ij}(\text{NP}) = \frac{\pi}{\sqrt{2}\alpha G_F V_{tb} V_{ts}^*} \frac{(g_1 + g_2)}{\Lambda_{\text{NP}}^2} X^{23} Y^{ij} \,, \tag{3.4}$$

$$C_L^{ij}(\text{NP}) = \frac{\pi}{\sqrt{2}\alpha G_F V_{tb} V_{ts}^*} \frac{(g_1 - g_2)}{\Lambda_{\text{NP}}^2} X^{23} Y^{ij} \,, \tag{3.5}$$

$$C_V^{ij}(\text{NP}) = -\frac{1}{2\sqrt{2}G_F V_{cb}} \frac{2g_2}{\Lambda_{\text{NP}}^2} \left(V_{cs} X^{23} + V_{cb} X^{33}\right) Y^{ij} \,. \tag{3.6}$$

In the following subsections we examine the experimentally-preferred values of the above quantities.

3.1.1 $C_9^{\mu\mu}(\text{NP}) = -C_{10}^{\mu\mu}(\text{NP})$

A global analysis of the $b \to s\ell^+\ell^-$ anomalies was recently performed in ref. [10]. The fit included data on $B \to K^{(*)}\mu^+\mu^-$, $B \to K^{(*)}e^+e^-$, $B_s^0 \to \phi\mu^+\mu^-$, $B \to X_s\mu^+\mu^-$, $b \to s\gamma$ and $B_s^0 \to \mu^+\mu^-$. It was found that there is a significant disagreement with the SM, possibly as large as 4σ, and that it can be explained if there is NP in $b \to s\mu^+\mu^-$. There are four possible explanations, each having roughly equal goodness-of-fits: (i) $C_9^{\mu\mu}(\text{NP}) < 0$, (ii) $C_9^{\mu\mu}(\text{NP}) = -C_{10}^{\mu\mu}(\text{NP}) < 0$, (iii) $C_9^{\mu\mu}(\text{NP}) = -C_9'^{\mu\mu}(\text{NP}) < 0$, and (iv) $C_9^{\mu\mu}(\text{NP}) = -C_{10}^{\mu\mu}(\text{NP}) = -C_9'^{\mu\mu}(\text{NP}) = -C_{10}'^{\mu\mu}(\text{NP}) < 0$. Of these, it is solution (ii) that interests us. According to the fit, the allowed 3σ range for the Wilson coefficients is

$$-1.13 \leq C_9^{\mu\mu}(\text{NP}) = -C_{10}^{\mu\mu}(\text{NP}) \leq -0.21 \,. \tag{3.7}$$

Note that the above range of the NP contribution is consistent with the R_K anomaly: the central value of R_K^{expt} can be explained with $C_9^{\mu\mu}(\text{NP}) \simeq -0.55$.

3.1.2 $C_L^{ij}(\text{NP})$

$C_L^{ij}(\text{NP})$ can be constrained by the existing data of $\bar{B} \to K\nu\bar{\nu}$ and $\bar{B} \to K^*\nu\bar{\nu}$ decays. The BaBar and Belle Collaborations give the following 90% C.L. upper limits [45, 46]:

$$\mathcal{B}\left(B^+ \to K^+\nu\bar{\nu}\right) \leq 1.7 \times 10^{-5} \,,$$
$$\mathcal{B}\left(B^+ \to K^{*+}\nu\bar{\nu}\right) \leq 4.0 \times 10^{-5} \,,$$
$$\mathcal{B}\left(B^0 \to K^{*0}\nu\bar{\nu}\right) \leq 5.5 \times 10^{-5} \,. \tag{3.8}$$

In ref. [59], these are compared with the SM predictions

$$\mathcal{B}_K^{\text{SM}} \equiv \mathcal{B}\left(B \to K\nu\bar{\nu}\right)_{\text{SM}} = (3.98 \pm 0.43 \pm 0.19) \times 10^{-6} \,,$$
$$\mathcal{B}_{K^*}^{\text{SM}} \equiv \mathcal{B}\left(B \to K^*\nu\bar{\nu}\right)_{\text{SM}} = (9.19 \pm 0.86 \pm 0.50) \times 10^{-6} \,. \tag{3.9}$$

Taking into account the theoretical uncertainties [59], the 90% C.L. upper bounds on the NP contributions are

$$\frac{\mathcal{B}_K^{\text{SM+NP}}}{\mathcal{B}_K^{\text{SM}}} \leq 4.8 \,, \qquad \frac{\mathcal{B}_{K^*}^{\text{SM+NP}}}{\mathcal{B}_{K^*}^{\text{SM}}} \leq 4.9 \,. \tag{3.10}$$

We have

$$\frac{\mathcal{B}_K^{\mathrm{SM+NP}}}{\mathcal{B}_K^{\mathrm{SM}}} = \frac{\mathcal{B}_{K^*}^{\mathrm{SM+NP}}}{\mathcal{B}_{K^*}^{\mathrm{SM}}} = \frac{1}{3|C_L^{\mathrm{SM}}|^2} \left(3|C_L^{\mathrm{SM}}|^2 + 2C_L^{\mathrm{SM}} \sum_{i=1}^{3} \mathrm{Re}[C_L^{ii}(\mathrm{NP})] + \sum_{i,j=1}^{3} |C_L^{ij}(\mathrm{NP})|^2 \right), \tag{3.11}$$

where $C_L^{\mathrm{SM}} \simeq -1.47/\sin^2\theta_W \simeq -6.36$ (θ_W is the Weinberg angle). The bound on NP therefore becomes

$$-13 \sum_{i=1}^{3} \mathrm{Re}[C_L^{ii}(\mathrm{NP})] + \sum_{i,j=1}^{3} |C_L^{ij}(\mathrm{NP})|^2 \leq 473. \tag{3.12}$$

A constraint on the NP contribution can also be obtained from the inclusive decay. The ALEPH Collaboration gives the 90% C.L. upper limit as $\mathcal{B}(B \to X_s \nu\bar{\nu}) \leq 6.4 \times 10^{-4}$ [60]. However, this implies $\mathcal{B}_{X_s}^{\mathrm{SM+NP}}/\mathcal{B}_{X_s}^{\mathrm{SM}} \leq 22$, which is a weaker constraint than that from the exclusive decays.

3.1.3 $C_V^{\ell\nu}(\mathrm{NP})$

The constraint on C_V^{ij} can be obtained from the comparison of the measurements of the ratios $R_{D^{(*)}} \equiv \mathcal{B}(\bar{B} \to D^{(*)}\tau^-\bar{\nu}_\tau)/\mathcal{B}(\bar{B} \to D^{(*)}\ell^-\bar{\nu}_\ell)$ ($\ell = e, \mu$) with their SM expectations. This is shown in eq. (1.2), and leads to the 3σ bounds

$$0.79 \leq R_D^{\mathrm{ratio}} \leq 1.79 \;, \quad 1.02 \leq R_{D^*}^{\mathrm{ratio}} \leq 1.53, \tag{3.13}$$

where

$$R_D^{\mathrm{ratio}} = R_{D^*}^{\mathrm{ratio}} = \frac{2 \left(\left|1 + C_V^{\tau\nu_\tau}(\mathrm{NP})\right|^2 + \sum_{j=1,2} \left|C_V^{\tau\nu_j}(\mathrm{NP})\right|^2 \right)}{1 + \left|1 + C_V^{\mu\nu_\mu}(\mathrm{NP})\right|^2 + \sum_{j=1,3} \left|C_V^{\mu\nu_j}(\mathrm{NP})\right|^2}. \tag{3.14}$$

Here we have assumed $C_V^{e\nu_j}(\mathrm{NP}) = 0$.

3.2 $\tau \to \mu\phi$

The NP effective Lagrangian of eq. (2.6) generates the process $\tau \to \mu s\bar{s}$:

$$\mathcal{L}_{\mathrm{eff}} = \frac{g_1 + g_2}{\Lambda_{\mathrm{NP}}^2} X^{22} Y^{23} \left(\bar{s}_L \gamma^\mu s_L\right) \left(\bar{\tau}_L \gamma_\mu \mu_L\right), \tag{3.15}$$

which will lead to $\tau \to \mu\phi$ and $\tau \to \mu\eta^{(\prime)}$. Writing the hadronic currents as

$$\langle 0|\bar{s}\gamma^\mu s|\phi\rangle = f_\phi m_\phi \epsilon_\phi^\mu, \quad \langle 0|\bar{s}\gamma^\mu s|\eta^{(\prime)}\rangle = i f_{\eta^{(\prime)}} p_{\eta^{(\prime)}}^\mu, \tag{3.16}$$

the branching ratios (neglecting the mass of the muon) are given by

$$\mathcal{B}(\tau \to \mu\phi) = \frac{f_\phi^2 m_\tau^3 \tau_\tau}{128\pi \Lambda_{\mathrm{NP}}^4} |\kappa|^2 \left(1 - \eta_\phi^2\right)^2 \left(1 + 2\eta_\phi^2\right),$$

$$\mathcal{B}(\tau \to \mu\eta^{(\prime)}) = \frac{f_{\eta^{(\prime)}}^2 m_\tau^3 \tau_\tau}{128\pi \Lambda_{\mathrm{NP}}^4} |\kappa|^2 \left(1 - \eta_{\eta^{(\prime)}}^2\right), \tag{3.17}$$

where $\kappa = (g_1 + g_2)X^{22}Y^{23}$, $\eta_\phi \equiv m_\phi/m_\tau$ and $\eta_\eta^{(\prime)} \equiv m_\eta^{(\prime)}/m_\tau$. Thus we obtain the following ratio:

$$\frac{\mathcal{B}\left(\tau \to \mu\eta^{(\prime)}\right)}{\mathcal{B}(\tau \to \mu\phi)} = \frac{f_{\eta^{(\prime)}}^2}{f_\phi^2} \cdot \frac{1 - \eta_{\eta^{(\prime)}}^2}{\left(1 - \eta_\phi^2\right)^2 \left(1 + 2\eta_\phi^2\right)} . \tag{3.18}$$

We may use the following expression to estimate f_ϕ^2:

$$f_\phi^2 = \frac{27 m_\phi \Gamma_\phi \mathcal{B}(\phi \to \mu^+\mu^-)}{4\pi\alpha_{\text{em}}^2} . \tag{3.19}$$

Taking the values for m_ϕ, m_τ, τ_τ, Γ_ϕ and $\mathcal{B}(\phi \to \mu^+\mu^-)$ from ref. [61], this yields $f_\phi \approx$ 225 MeV. For the $\eta^{(\prime)}$ decay constant we get (using $f_\pi = 130\,\text{MeV}$, $f_1 \sim 1.1 f_\pi$, $f_8 \sim 1.3 f_\pi$ [62], and $\theta = 19.5°$ [63])

$$f_\eta = -\frac{f_\pi}{\sqrt{3}} \left(\sqrt{2} \cos\theta \frac{f_8}{f_\pi} + \sin\theta \frac{f_1}{f_\pi} \right) \simeq -157.63\,\text{MeV} ,$$

$$f_{\eta'} = \frac{f_\pi}{\sqrt{3}} \left(\cos\theta \frac{f_1}{f_\pi} - \sqrt{2} \sin\theta \frac{f_8}{f_\pi} \right) \simeq 31.76\,\text{MeV} . \tag{3.20}$$

Using these we obtain

$$\frac{\mathcal{B}(\tau \to \mu\eta)}{\mathcal{B}(\tau \to \mu\phi)} \sim 0.60 , \quad \frac{\mathcal{B}(\tau \to \mu\eta')}{\mathcal{B}(\tau \to \mu\phi)} \sim 1.9 \times 10^{-2} . \tag{3.21}$$

The current 90% C.L. limits on these branching ratios are [61]

$$\mathcal{B}(\tau \to \mu\eta) < 6.5 \times 10^{-8} ,$$
$$\mathcal{B}(\tau \to \mu\eta') < 1.3 \times 10^{-7} ,$$
$$\mathcal{B}(\tau \to \mu\phi) < 8.4 \times 10^{-8} . \tag{3.22}$$

Of these decays, $\tau \to \mu\eta'$ is the least constraining. And since $\tau \to \mu\phi$ and $\tau \to \mu\eta$ are of the same order, we will use $\tau \to \mu\phi$ to constrain the coupling κ. Using $\mathcal{B}(\tau \to \mu\phi) < 8.4 \times 10^{-8}$ [64] and $\Lambda_{\text{NP}} = 1\,\text{TeV}$, we obtain the constraint

$$|\kappa| < 0.019 . \tag{3.23}$$

3.3 B_s^0-$\bar{B}_s^0$ mixing

As noted in section 2.1, the VB model also generates four-quark operators at tree level. In the mass basis, the operator of eq. (2.13) includes

$$\frac{(g_{qV}^{33})^2}{2m_V^2} \sin^2\theta_D \cos^2\theta_D \left(\bar{s}_L \gamma^\mu b_L\right)\left(\bar{s}_L \gamma_\mu b_L\right) . \tag{3.24}$$

This generates a contribution to B_s^0-$\bar{B}_s^0$ mixing. In the SM, the same operator is produced via a box diagram. Here we have

$$N C_{VLL}^{\text{SM}} \left(\bar{s}_L \gamma^\mu b_L\right)\left(\bar{s}_L \gamma_\mu b_L\right) , \tag{3.25}$$

where

$$N = \frac{G_F^2 m_W^2}{16\pi^2} \left(V_{tb}V_{ts}^*\right)^2 \sim 10^{-11}\,\text{GeV}^{-2}\,,$$

$$C_{VLL}^{\text{SM}} = \eta_{B_s} x_t \left[1 + \frac{9}{1-x_t} - \frac{6}{(1-x_t)^2} - \frac{6x_t^2 \ln x_t}{(1-x_t)^3}\right]. \tag{3.26}$$

In the above, $x_t \equiv m_t^2/m_W^2$ and $\eta_{B_s} = 0.551$ is the QCD correction [65]. The SM and NP contributions can be combined. We define

$$NC_{VLL} \equiv NC_{VLL}^{\text{SM}} + \frac{\left(g_{qV}^{33}\right)^2}{2m_V^2} \sin^2\theta_D \cos^2\theta_D\,. \tag{3.27}$$

The mass difference in the B_s system is then given by

$$\Delta M_s = \frac{2}{3} m_{B_s} f_{B_s}^2 \hat{B}_{B_s} |NC_{VLL}|\,. \tag{3.28}$$

Taking $f_{B_s}\sqrt{\hat{B}_{B_s}} = (266 \pm 18)\,\text{MeV}$ [66, 67], $V_{tb}V_{ts}^* = -0.0405 \pm 0.0012$ [61, 68], and $\overline{m}_t = 160\,\text{GeV}$ [61, 69], we find the SM prediction

$$\Delta M_s^{\text{SM}} = (17.4 \pm 2.6)\,\text{ps}^{-1}\,. \tag{3.29}$$

This is to be compared with the experimental measurement [70]

$$\Delta M_s = (17.757 \pm 0.021)\,\text{ps}^{-1}\,. \tag{3.30}$$

As we will see in the next section, the constraint on the VB model from B_s^0-$\bar{B}_s^0$ mixing is extremely stringent.

3.4 $\tau \to 3\mu$

Finally, the VB model also produces four-lepton operators at tree level. In the mass basis, the Lagrangian of eq. (2.13) includes the operator

$$-\frac{(g_{\ell V}^{33})^2}{2m_V^2} \sin^3\theta_L \cos\theta_L \left(\bar{\mu}_L\gamma^\mu\tau_L\right)\left(\bar{\mu}_L\gamma_\mu\mu_L\right)\,, \tag{3.31}$$

which generates the decay $\tau \to 3\mu$. As this is a lepton-flavor-violating decay, it can arise only due to NP. The decay rate for $\tau \to 3\mu$ is then given by

$$\mathcal{B}\left(\tau^- \to \mu^-\mu^+\mu^-\right) = X \frac{\left(g_{\ell V}^{33}\right)^4}{16 m_V^4} \frac{m_\tau^5 \tau_\tau}{192\pi^3} \sin^6\theta_L \cos^2\theta_L\,, \tag{3.32}$$

where X is a suppression factor due to the non-zero muon mass. In terms of $\eta_\mu = m_\mu/m_\tau$, it is given by

$$X = 12 \int\limits_{4\eta_\mu^2}^{(1-\eta_\mu)^2} \frac{dx}{\sqrt{x}} \left(x - 2\eta_\mu^2\right)\left(1 + \eta_\mu^2 - x\right) \sqrt{\left(x - 4\eta_\mu^2\right)\left(1 - 2\left(x + \eta_\mu^2\right) + \left(x + \eta_\mu^2\right)^2\right)}$$

$$\approx 0.94\,. \tag{3.33}$$

At present, the branching ratio for $\tau^- \to \mu^- \mu^+ \mu^-$ has only an experimental upper bound [71]:

$$\mathcal{B}\left(\tau^- \to \mu^- \mu^+ \mu^-\right) < 2.1 \times 10^{-8} \text{ at } 90\% \text{ C.L.} \tag{3.34}$$

This then puts a constraint on θ_L in the VB model, which, as we will see in the next section, is quite strong.

4 Models: allowed parameter space

Taking into account all the experimental constraints described in section 3, we find the allowed parameter space in the four NP models. We assume $\Lambda_{\text{NP}} = 1\,\text{TeV}$, and take the third-generation coupling to be $2g_{qV}^{33} g_{\ell V}^{33} = \left|h_{U_1}^{33}\right|^2 = \left|h_{U_3}^{33}\right|^2 = \left|h_{S_3}^{33}\right|^2 = 1$. For the VB model, we take $g_{qV}^{33} = g_{\ell V}^{33}$. (In the next section we vary g_{qV}^{33} and $g_{\ell V}^{33}$.) In figure 1, the constraints in the (θ_L, θ_D) plane are shown for the VB, U_1, U_3 and S_3 models. These are presented only for $\theta_L \geq 0$; the space is symmetric under $\theta_L \to -\theta_L$.

For all four models, the flavor anomalies R_D, R_{D^*} and R_K can be explained in the shaded regions colored in pink, red and blue, respectively. The gray shaded region is allowed from $\bar{B} \to K^{(*)} \nu \bar{\nu}$ at 90% C.L. The region bounded by the green lines is consistent with the 90% C.L. upper limit on the branching ratio of $\tau \to \mu \phi$. For the VB model, there are additional constraints coming from B_s^0-$\bar{B}_s^0$ mixing and $\tau \to 3\mu$. For the $\tau \to 3\mu$ constraint, the region to the left of the cyan line is allowed. The B_s^0-$\bar{B}_s^0$ mixing constraint is shown in the orange region, which is extremely narrow near $\theta_D = 0, \pi/2$.

Based on this figure, one can make two observations:

- There are only two regions in parameter space where the constraints from R_D, R_{D^*}, R_K and $\bar{B} \to K^{(*)} \nu \bar{\nu}$ (if applicable) might overlap. These are roughly around $\pi/16 \lesssim \theta_L \lesssim \pi/8$, with θ_D near 0 (region 1) or $\pi/2$ (region 2). However, the additional constraint from $\tau \to \phi \mu$ distinguishes the two regions. That is, while region 1 satisfies the $\tau \to \phi \mu$ constraint, region 2 does not, and is therefore excluded. Henceforth, we focus only on region 1.

- For the VB model, the constraint from B_s^0-$\bar{B}_s^0$ mixing has the same shape as that from $\bar{B} \to K^{(*)} \nu \bar{\nu}$. They are both independent of θ_L, and so bound only θ_D. However, we see that the B_s^0-$\bar{B}_s^0$ mixing constraint is much more stringent than that from $\bar{B} \to K^{(*)} \nu \bar{\nu}$. For $g_{qV}^{33} = g_{\ell V}^{33} = 1/\sqrt{2}$, one has $|\theta_D| \ll 1$, so that it is somewhat difficult from this figure to determine if this region is consistent with the others.

In order to obtain more information, in figure 2, we show the constraints in region 1 of the (θ_L, θ_D) plane for the VB, S_3, U_1, and U_3 models. In the figures, we indicate the values of the contours for the flavor anomalies, that is, $R_X^{\text{NP+SM}}/R_X^{\text{SM}}$ for $X = K$ and $D^{(*)}$. From this figure, we can see that

- For the S_3 model, the R_{D^*} region does not overlap with the R_K or $\bar{B} \to K^{(*)} \nu \bar{\nu}$ regions. And for the U_3 model, the R_{D^*} and $\bar{B} \to K^{(*)} \nu \bar{\nu}$ regions do not overlap. Therefore, S_3 and U_3 with the flavor mixing structure of eq. (2.5) are excluded.[4]

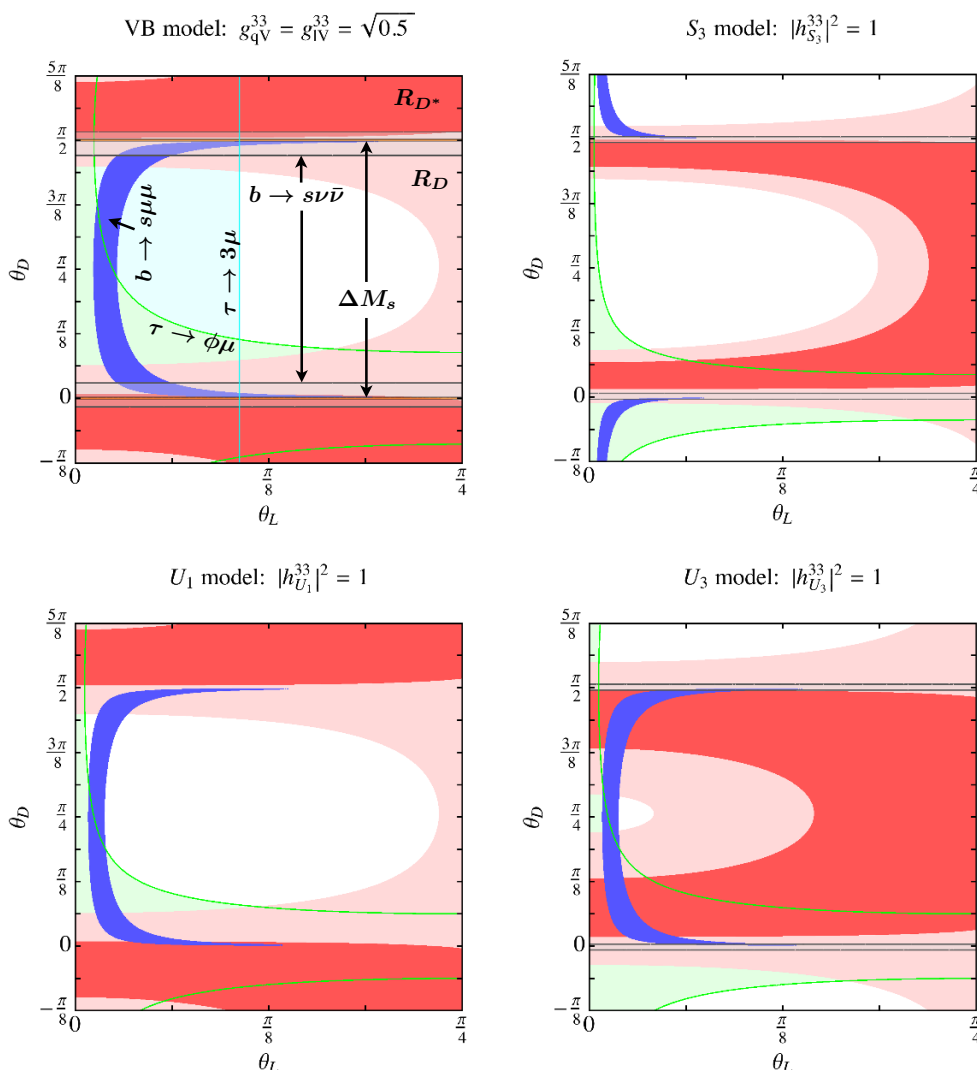[4] A different type of the mixing for the U_3 LQ is discussed in ref. [57].

Figure 1. Allowed regions in the (θ_L, θ_D) plane for the VB, S_3, U_1, and U_3 models. We have fixed the NP scale as $\Lambda_{\rm NP} = 1\,{\rm TeV}$. In each model, the third-generation coupling is taken as $2g_{qV}^{33} g_{\ell V}^{33} = \left|h_{U_1}^{33}\right|^2 = \left|h_{U_3}^{33}\right|^2 = \left|h_{S_3}^{33}\right|^2 = 1$. The R_D, R_{D^*} and R_K (along with the $b \to s\ell^+\ell^-$ data) anomalies can be explained in the shaded regions colored in pink, red, and blue, respectively. The regions bounded by the gray, green, cyan, and orange lines are allowed from the measurements of $b \to s\nu\bar{\nu}$, $\tau \to \mu\phi$, $\tau \to 3\mu$, and ΔM_s, respectively. The last two observables are applicable only in the VB model.

- For the U_1 model, if $\theta_D \leq 0.028$, there is a region where all the constraints overlap, and so this model is allowed. On the other hand, the VB model is on the edge of exclusion — the boundaries of the ΔM_s, $b \to s\mu\mu$, and $\tau \to 3\mu$ constraints are touching, but just barely. This also implies that the VB model only allows limited values of these observables. From this figure we see that $\tau \to 3\mu$ is a critical process for the VB model. Therefore, in addition to the 90% C.L. upper bound on $\mathcal{B}(\tau^- \to \mu^-\mu^+\mu^-)$ from eq. (3.34) shown in the figure (solid cyan line), we superpose an estimated 3σ upper limit on this branching ratio (dashed cyan line).
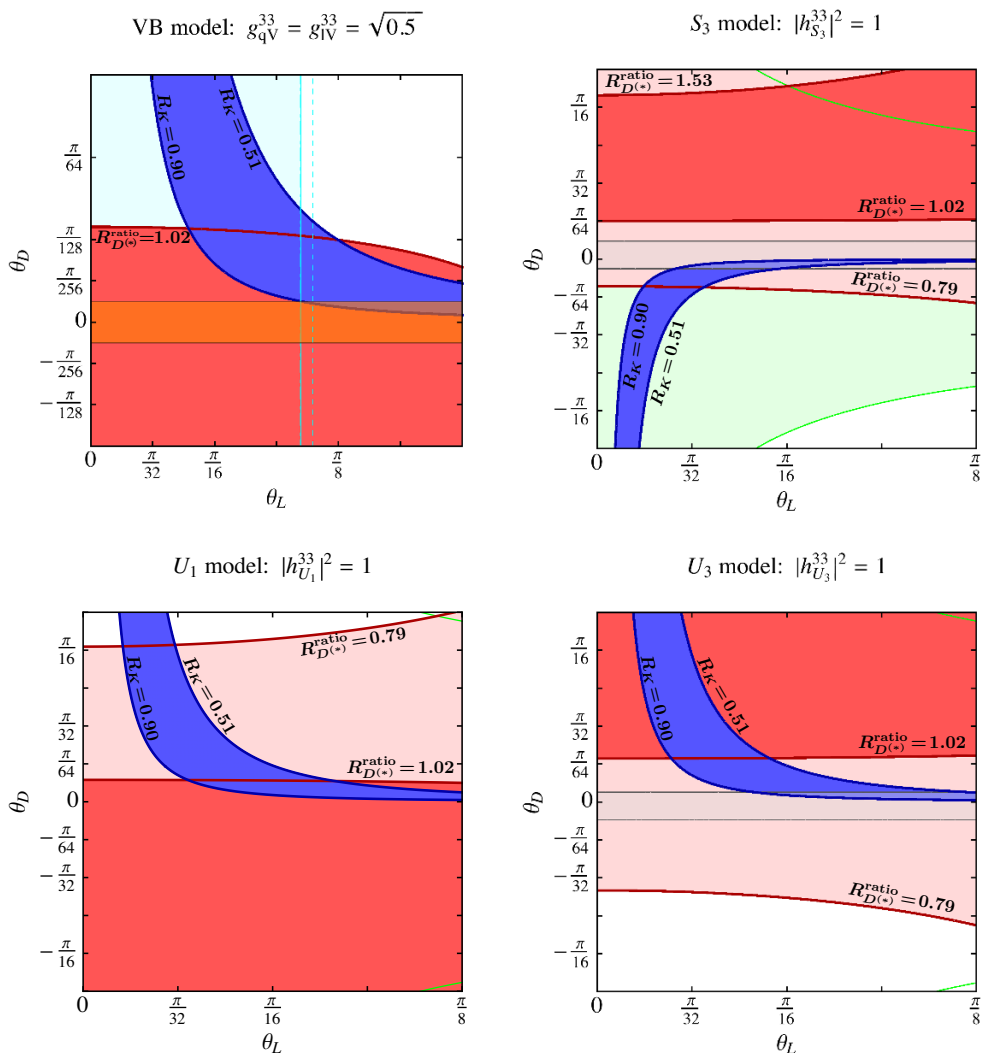
Figure 2. Magnified figures of figure 1. The color legends are the same as the previous figures. The values of the contours for $R_X^{\text{NP+SM}}/R_X^{\text{SM}}$ ($X = K, D, D^*$) are indicated. The R_D constraint (in pink) is satisfied for the entire region of the plot in VB and hence omitted.

- Comparing the VB and U_1 models, the constraints from the flavor anomalies (R_K, $R_{D^{(*)}}$) are similar (for θ_D near 0). But the additional constraints from ΔM_s and $\tau \to 3\mu$ put VB on the verge of exclusion. The limited amount of parameter space available to VB increases its predictive power. Specifically, while the allowed region for the U_1 model includes $0.11 \leq \theta_L \leq 0.73$ and $0.001 \leq \theta_D \leq 0.028$, for the VB model (θ_L, θ_D) is limited to be $\simeq (0.333, 0.006)$.

The VB and U_1 models are therefore the candidates to simultaneously explain the R_K and $R_{D^{(*)}}$ puzzles in the case where the NP couples predominantly to the third-generation fermions.

5 Predictions

We have now established that the VB and U_1 models are candidates to explain the present discrepancies with the SM in $b \to s\mu^+\mu^-$, $R_{D^{(*)}}$ and R_K. The main question we wish to address in this paper is: is there any way of distinguishing the two models? There are two handles that can potentially accomplish this. First, the VB model contributes to four-lepton and four-quark operators, and hence to processes such as $\tau \to 3\mu$ and B_s^0-$\bar{B}_s^0$ mixing, while the U_1 model does not.[5] Second, due to additional constraints, the allowed region in (θ_L, θ_D) space is essentially a single point for VB, while it is much larger for U_1. Below we explore the predictions of the two models for various processes. As we will see, it is potentially possible to distinguish the VB and U_1 models.

5.1 Processes

5.1.1 $R_{D^{(*)}}$

The 3σ allowed ranges of $R_{D^{(*)}}^{\mathrm{ratio}}$ are given in eq. (3.13). At present, large deviations from the SM are allowed (up to 79% and 53% for R_D and R_{D^*}, respectively). On the other hand, from figure 2, we see that the VB and U_1 models are allowed only if θ_D is very small. This means that such large deviations in $R_{D^{(*)}}$ from the SM are not favored, as these are inconsistent with the R_K anomaly. The models predict

$$
\begin{aligned}
VB &: \quad R_{D^{(*)}}^{\mathrm{ratio}} \simeq 1.04 \,, \\
U_1 &: \quad 1.02 \le R_{D^{(*)}}^{\mathrm{ratio}} \le 1.05 \,.
\end{aligned}
\tag{5.1}
$$

Thus, even if $R_{D^{(*)}}$ is measured with greater precision, it will probably not be possible to distinguish the VB and U_1 models. However, if the measurements confirm large deviations from the SM, both models will be ruled out.

5.1.2 R_K

The situation is different for R_K. Using eq. (1.1), its allowed 3σ range is $0.498 \le R_K \le 1.036$. The models predict [73]

$$
\begin{aligned}
VB &: \quad R_K \simeq 0.90 \,, \\
U_1 &: \quad 0.51 \le R_K \le 0.90 \,.
\end{aligned}
\tag{5.2}
$$

We therefore see that the U_1 model can accomodate smaller values of R_K than can the VB model. This is due to the fact that its allowed (θ_L, θ_D) region includes larger values of θ_L. Thus, if future measurements of R_K find it to be less than 0.90 at higher than 90% C.L., this would point clearly to U_1 (and exclude VB).

---

[5]In this paper we perform the analysis at tree level. Radiative corrections to four-lepton operators have been considered in ref. [72] within an EFT framework. However, as with all EFT analyses, the results do not necessarily apply to all models. To obtain the proper result, a more complete analysis must be done within each individual model.

5.1.3 $\tau \to 3\mu$

This decay is particularly interesting because only the VB model contributes to it. The present experimental bound is $\mathcal{B}(\tau^- \to \mu^- \mu^+ \mu^-) < 2.1 \times 10^{-8}$ at 90% C.L. [eq. (3.34)]. Belle II expects to reduce this limit to $< 10^{-10}$ [74]. The reach of LHCb is somewhat weaker, $< 10^{-9}$ [75].

Now, the amplitude for $\tau \to 3\mu$ depends only on θ_L [eq. (3.31)]. In figure 2, we see that the allowed value of θ_L corresponds to the present experimental bound. That is, VB predicts

$$\mathcal{B}(\tau^- \to \mu^- \mu^+ \mu^-) \simeq 2.1 \times 10^{-8}. \tag{5.3}$$

Thus, the VB model predicts that $\tau \to 3\mu$ should be observed at both LHCb and Belle II. This is a smoking-gun signal for the model.

5.1.4 $B \to K^{(*)}\mu\tau$

The BaBar Collaboration obtained an experimental bound of $\mathcal{B}(B^+ \to K^+ \mu^\pm \tau^\mp) < 4.8 \times 10^{-5}$ at 90% C.L. [76]. Belle II will collect 100 times more data than BaBar, and this will allow it to measure $\mathcal{B}(B^+ \to K^+ \mu^\pm \tau^\mp)$ to a level of 5×10^{-7} [77].

The models predict [73]

$$
\begin{aligned}
VB \quad &: \quad \mathcal{B}\left(B \to K^{(*)}\mu\tau\right) \simeq 4.0 \times 10^{-10}, \\
U_1 \quad &: \quad 6.8 \times 10^{-11} \le \mathcal{B}\left(B \to K^{(*)}\mu\tau\right) \le 2.1 \times 10^{-8}.
\end{aligned} \tag{5.4}
$$

Neither model can produce $\mathcal{B}(B \to K^{(*)}\mu\tau)$ sufficiently large that it can be observed at Belle II.

5.1.5 $B \to K^{(*)}\tau^+\tau^-$

The BaBar Collaboration recently put a limit of $\mathcal{B}(B^+ \to K^+ \tau^+ \tau^-) < 2.25 \times 10^{-3}$ at 90% C.L. [78]. Belle II will be able to improve on this, but because there are two τ's in the final state, the expected reach is only $\sim 2 \times 10^{-4}$ [77].

To measure and calculate the branching ratio of $B \to K^{(*)}\tau^+\tau^-$, we need to deal with charmonium resonances. In analogy with $B \to K^{(*)}\mu^+\mu^-$, we take $q^2 > 15\,\text{GeV}^2$ for integration and obtain the partial branching ratio by using `flavio` [73]:

$$
\begin{aligned}
VB \quad &: \quad \mathcal{B}\left(B \to K^{(*)}\tau^+\tau^-\right) \simeq 4.4 \times 10^{-8}, \\
U_1 \quad &: \quad 7.6 \times 10^{-10} \le \mathcal{B}\left(B \to K^{(*)}\tau^+\tau^-\right) \le 1.5 \times 10^{-6}.
\end{aligned} \tag{5.5}
$$

The values of $\mathcal{B}(B \to K^{(*)}\tau^+\tau^-)$ possible in both models are at least two orders of magnitude smaller than the estimated reach of Belle II. This decay can therefore not be used as a signal of the VB and/or U_1 models.

5.1.6 $B_s^0 \to \mu\tau$, $B_s^0 \to \tau^+\tau^-$

At present, LHCb is working on measuring these two decays, which are difficult due to the presence of τ's in the final state. However, no estimates of the reach are available [79]. (At Belle II, a rough estimate for $B_s^0 \to \tau^+\tau^-$ could be $\sim 2 \times 10^{-3}$ with $50\,\mathrm{ab}^{-1}$ of data, obtained by rescaling the present data at Belle.)

For $B_s^0 \to \mu\tau$, the models predict

$$
\begin{aligned}
VB \quad &: \quad \mathcal{B}\left(B_s^0 \to \mu\tau\right) \simeq 6.7 \times 10^{-9}\,, \\
U_1 \quad &: \quad 1.1 \times 10^{-9} \le \mathcal{B}\left(B_s^0 \to \mu\tau\right) \le 3.6 \times 10^{-7}\,,
\end{aligned}
\tag{5.6}
$$

while for $B_s^0 \to \tau^+\tau^-$ we have

$$
\begin{aligned}
VB \quad &: \quad \mathcal{B}\left(B_s^0 \to \tau^+\tau^-\right) \simeq 2.4 \times 10^{-7}\,, \\
U_1 \quad &: \quad 5.8 \times 10^{-18} \le \mathcal{B}\left(B_s^0 \to \tau^+\tau^-\right) \le 6.7 \times 10^{-6}\,.
\end{aligned}
\tag{5.7}
$$

For $B_s^0 \to \mu\tau$, if the branching ratio were measured to be between 6.7×10^{-9} and 3.6×10^{-7}, this would point to the U_1 model. However, it is unlikely that such a small branching ratio is measurable. Similarly, if $\mathcal{B}(B_s^0 \to \tau^+\tau^-)$ were found to be in the range 2.4×10^{-7}–6.7×10^{-6}, this would indicate U_1. However, here too it is not clear that such a small branching ratio is measurable.

5.1.7 $\Upsilon \to \mu\tau$

Finally, we turn to $\Upsilon \to \mu\tau$. This lepton-flavor-violating decay has been overlooked in previous analyses, but it is potentially an important process to consider.[6] At the fermion level, this decay is $b\bar{b} \to \mu\tau$, and it can receive contributions from both the VB and U_1 models. Note that this process has a pattern of mixing different from the above processes, and thus the models provide unique predictions.

In the past, the BaBar [81] and CLEO [82] Collaborations have studied lepton flavor violation in narrow $\Upsilon(nS)(n=1,2,3)$ decays. The strongest limits come from BaBar [81], which put an upper limit on $\mathcal{B}(\Upsilon(2S,3S) \to \mu\tau)$ of a few times 10^{-6}. This was obtained using $13.6\,\mathrm{fb}^{-1}$ and $26.8\,\mathrm{fb}^{-1}$ of the BaBar dataset on the $\Upsilon(2S)$ and $\Upsilon(3S)$, respectively. Belle II is expected to collect a few hundred fb^{-1} of data on the $\Upsilon(3S)$ [77]. A precise estimate of the sensitivity to $\Upsilon(3S) \to \mu\tau$ will require a dedicated study. However, given the order-of-magnitude increase in luminosity at Belle II compared to BaBar, we expect roughly an order-of-magnitude improvement in the sensitivity. That is, a reach of about 10^{-7} for $\mathcal{B}(\Upsilon(3S) \to \mu\tau)$ at Belle II is not unreasonable. These decays may also be studied at LHCb, but we are not aware of the LHCb reach for these processes.

In the SM, the LFV decay $\Upsilon(nS) \to \ell^-\ell'^+$, where ℓ and ℓ' represent leptons of different flavor, is highly suppressed. On the other hand, in the VB and U_1 models, $\Upsilon(nS) \to \mu^-\tau^+$ receives significant contributions. Assuming the NP is purely left-handed, the decay rate for this process is given by

$$
\Gamma\left(\Upsilon(nS) \to \mu^-\tau^+\right) = \frac{m_{\Upsilon(nS)}^3 f_{\Upsilon(nS)}^2}{48\pi}\left(1-\eta_\tau^2\right)\left(2-\eta_\tau^2-\eta_\tau^4\right)|\kappa|^2\,,
\tag{5.8}
$$

---

[6]Quark flavor violating quarkonium decays were considered in ref. [80].

where $\eta_\tau = m_\tau/m_{\Upsilon(nS)}$ and κ contains the coupling corresponding to the transition $b\bar{b} \to \tau\mu$. In the VB and U_1 models we have

$$\kappa = -\frac{g_1 + g_2}{2\Lambda_{\rm NP}^2} X^{33} Y^{32} = \frac{g_1 + g_2}{2\Lambda_{\rm NP}^2} \cos^2 \theta_D \cos \theta_L \sin \theta_L \,. \tag{5.9}$$

The decay constant $f_{\Upsilon(nS)}$ can be found using the electromagnetic decay $\Upsilon(nS) \to \ell^-\ell^+$, which is unaffected by NP. Its decay rate can be expressed as

$$\Gamma\left(\Upsilon(nS) \to \ell^-\ell^+\right) = \frac{4\pi\alpha^2}{27} \frac{f_{\Upsilon(nS)}^2}{m_{\Upsilon(nS)}} \left(1 + 2\eta_{\ell(nS)}^2\right) \sqrt{1 - 4\eta_{\ell(nS)}^2} \,, \tag{5.10}$$

where $\eta_{\ell(nS)} = m_\ell/m_{\Upsilon(nS)}$.

We may now combine eqs. (5.8), (5.9) and (5.10) to get predictions for the branching ratio of $\Upsilon(nS) \to \mu\tau$ in the VB and U_1 models. These are

$$
\begin{aligned}
VB \quad &: \quad \mathcal{B}(\Upsilon(1S) \to \mu\tau) \simeq 2.3 \times 10^{-9} \,, \\
&\quad \mathcal{B}(\Upsilon(2S) \to \mu\tau) \simeq 2.3 \times 10^{-9} \,, \\
&\quad \mathcal{B}(\Upsilon(3S) \to \mu\tau) \simeq 3.0 \times 10^{-9} \,, \\
U_1 \quad &: \quad 1.1 \times 10^{-9} \leq \mathcal{B}(\Upsilon(1S) \to \mu\tau) \leq 2.4 \times 10^{-8} \,, \\
&\quad 1.2 \times 10^{-9} \leq \mathcal{B}(\Upsilon(2S) \to \mu\tau) \leq 2.4 \times 10^{-8} \,, \\
&\quad 1.5 \times 10^{-9} \leq \mathcal{B}(\Upsilon(3S) \to \mu\tau) \leq 3.2 \times 10^{-8} \,.
\end{aligned}
\tag{5.11}
$$

The VB model predicts a branching ratio of $O(10^{-9})$, while it can be $O(10^{-8})$ in the U_1 model. Therefore this mode can potentially allow us to distinguish between the two models. However, even the upper limit predicted by the U_1 model seems to be out of reach of Belle II, according to our estimate of its reach. On the other hand, perhaps Belle II or LHCb will in fact be sensitive to branching ratios of $O(10^{-8})$. Or perhaps the NP coupling is bigger than we have assumed (see section 5.2 below), resulting in larger branching ratios. The point is that $\Upsilon \to \mu\tau$ decays may provide us with valuable information in identifying the lepton-flavor-violating NP.

5.1.8 Summary

There are therefore three observables that can distinguish the VB and U_1 models:

1. $\tau \to 3\mu$: VB predicts $\mathcal{B}(\tau^- \to \mu^-\mu^+\mu^-) \simeq 2.1 \times 10^{-8}$, its present upper limit (U_1 does not contribute to the decay). This implies that the LFV decay $\tau \to 3\mu$, which is absent in the SM, should be observed at both LHCb and Belle II. This is therefore a smoking-gun signal: it can occur only in the VB model, and if the decay is not seen, the model would be ruled out.

2. R_K: the current 3σ range for R_K is $0.498 \leq R_K \leq 1.036$. The U_1 model can accomodate smaller values of R_K, while the VB model cannot. Specifically, if future measurements of R_K find it to be less than 0.90 at higher than 90% C.L., this would point to U_1 (and exclude VB).

3. $\Upsilon \to \mu\tau$: to date, the LFV decay $\Upsilon \to \mu\tau$ has been overlooked as a test of NP models in B decays. Within the VB model, $\mathcal{B}(\Upsilon(nS) \to \mu\tau)$ is a few times 10^{-9}, but in the U_1 model, it can reach a few times 10^{-8}. Belle II should be able to measure $\mathcal{B}(\Upsilon(3S) \to \mu\tau)$ down to $\sim 10^{-7}$. However, this is only a very rough estimate — a detailed study is needed for a precise determination of the reach. It may be that, in fact, Belle II (or LHCb) will be able to observe branching ratios of $O(10^{-8})$. And if the decay $\Upsilon \to \mu\tau$ is observed, this will suggest the U_1 model.

There are five other observables that receive contributions in the VB and U_1 models: $R_{D^{(*)}}$, $B \to K^{(*)}\mu\tau$, $B \to K^{(*)}\tau^+\tau^-$, $B_s^0 \to \mu\tau$, $B_s^0 \to \tau^+\tau^-$. However, either these observables cannot distinguish the two models, or, if they can, the predicted branching ratios fall below the expected reach of Belle II and LHCb.

5.2 Varying the couplings

Now, the results of the previous subsection have been found assuming that $2\, g_{qV}^{33} g_{\ell V}^{33} = \left| h_{U_1}^{33} \right|^2 = 1$. However, there is nothing special about this value of the square of the coupling (henceforth denoted coupling^2). This then raises the question: if the coupling^2 is allowed to take different values, how do the results of section 5.1 change? This is examined in this subsection.

For each new value of the coupling^2, one must redo the analysis of section 4, to determine the region in (θ_L, θ_D) parameter space allowed by the various experimental constraints. That is, figures of the type in figure 2 are produced. The following results are found:

- For the S_3 and U_3 models, it is found that the R_{D^*} and $\bar{B} \to K^{(*)}\nu\bar{\nu}$ regions do not overlap, and this is independent of the value of coupling^2. S_3 and U_3 are therefore excluded.

- For the VB model, the constraints essentially come from three observables:

  1. B_s^0-$\bar{B}_s^0$ mixing (ΔM_s): puts an upper bound on $g_{qV}^{33} \sin\theta_D \cos\theta_D$ [eq. (3.24)].
  2. $\tau \to 3\mu$: puts an upper bound on $(g_{\ell V}^{33})^2 \sin^3\theta_L \cos\theta_L$ [eq. (3.31)].
  3. $b \to s\mu^+\mu^-$ ($C_9^{\mu\mu}(\text{NP})$): puts a lower bound on $(g_{qV}^{33} \sin\theta_D \cos\theta_D)(g_{\ell V}^{33} \sin^2\theta_L)$. (There is also an upper bound, but this is not relevant for the VB model.)

  These three constraints overlap at basically a single point in the parameter space. However, one still has the freedom to relabel this point by adjusting the values of g_{qV}^{33}, $g_{\ell V}^{33}$, θ_L and θ_D. For example, in the previous section we had $g_{qV}^{33} = g_{\ell V}^{33} = \sqrt{0.5}$, $(\theta_L, \theta_D) = (0.333, 0.006)$. However, two other possibilities are $g_{qV}^{33} = \sqrt{0.5}/0.8$, $g_{\ell V}^{33} = 0.8\sqrt{0.5}$, $(\theta_L, \theta_D) = (0.392, 0.005)$ and $g_{qV}^{33} = \sqrt{0.28}/1.2$, $g_{\ell V}^{33} = 1.2\sqrt{0.28}$, $(\theta_L, \theta_D) = (0.360, 0.009)$. But the key point is that, in both of these cases, the predictions for other processes are little changed from those in section 5.1.

- The U_1 model is viable only if $\left| h_{U_1}^{33} \right|^2 \geq 0.5$. Values of the coupling^2 larger than 5 are allowed, see figure 3.
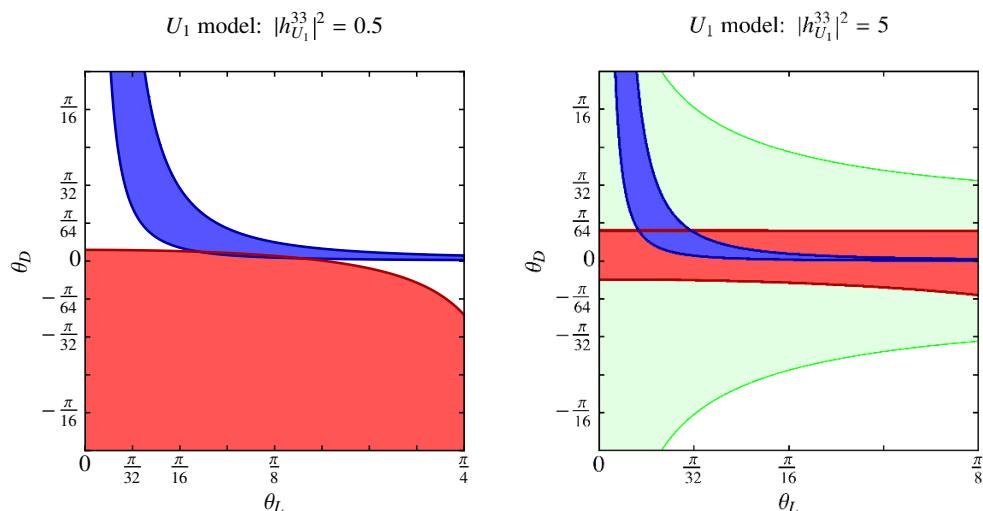
Figure 3. Figure 2 for the U_1 model, but with $\left|h^{33}_{U_1}\right|^2 = 0.5$ (left) or $\left|h^{33}_{U_1}\right|^2 = 5$ (right). Left: the blue (R_K) and red (R_{D^*}) regions barely overlap, so this is the minimum value of the coupling[2] for which U_1 is viable. Right: the regions overlap, so U_1 is viable for $\left|h^{33}_{U_1}\right|^2 = 5$ (as well as for larger values of the coupling[2]).

In fact, we do have some information about the value of the coupling[2]. One can set limits on coupling[2]$/\Lambda^2_{\text{NP}}$ from direct searches, assuming a certain mode of production for the new mediator states. Following ref. [83], using the $b\bar{b} \to \tau\bar{\tau}$ process mediated by s- or t-channel vector-boson or leptoquark exchange, one can get the following rough upper bounds: $|g^{33}_{qV} g^{33}_{\ell V}|_{\max}/\Lambda^2_{\text{NP}} \sim 3\,\text{TeV}^{-2}$ for the VB model and $\left|h^{33}_{U_1}\right|^2_{\max}/\Lambda^2_{\text{NP}} \sim 5\,\text{TeV}^{-2}$ for the U_1 model. That is, for $\Lambda_{\text{NP}} = 1\,\text{TeV}$, $g^{33}_{qV} g^{33}_{\ell V} \leq 3$ and $\left|h^{33}_{U_1}\right|^2 \leq 5$.[7]

In light of these results, we rederive the predictions of the U_1 model for the various observables, allowing $0.5 \leq \left|h^{33}_{U_1}\right|^2 \leq 5$. For comparison, we include the VB predictions from section 5.1. We find

1. $R_{D^{(*)}}$:

$$
\begin{aligned}
VB &: \quad R^{\text{ratio}}_{D^{(*)}} \simeq 1.04 \,, \\
U_1 &: \quad 1.02 \leq R^{\text{ratio}}_{D^{(*)}} \leq 1.29 \,.
\end{aligned}
\tag{5.12}
$$

For coupling[2] $= 1$, we found that, for both models, large deviations in $R_{D^{(*)}}$ from the SM are not favored, so it is not possible to distinguish the VB and U_1 models using $R_{D^{(*)}}$. From the above numbers, we see that, when the coupling[2] is allowed to vary, this no longer holds. If it is found that $1.04 < R_{D^{(*)}} \leq 1.29$, this will indicate U_1.

---

[7]To be precise, the bound given in ref. [83] should be applied as $g^{33}_{qV} g^{33}_{\ell V} \cos^2 \theta_D \cos^2 \theta_L \leq 3$ and $\left|h^{33}_{U_1} \cos\theta_D \cos\theta_L\right|^2 \leq 5$ (for $\Lambda_{\text{NP}} = 1\,\text{TeV}$). The down-sector mixing, which reduces the rate of $b\bar{b}$ pair production, is negligible since $\theta_D \ll 1$ for the present case. As for the lepton mixing, it can at most reduce the decay rate into $\tau\bar{\tau}$ by 15% (for $\theta_L \leq \pi/8$). Here we (conservatively) ignore this effect, resulting in a slightly more stringent constraint on coupling[2], as shown in the main text.

2. R_K:

$$VB \quad : \quad R_K \simeq 0.90 \,,$$
$$U_1 \quad : \quad 0.51 \le R_K \le 0.90 \,. \tag{5.13}$$

The result is as before: if future measurements find $0.51 \le R_K < 0.90$, this would point clearly to U_1 (and exclude VB).

3. $B \to K^{(*)}\mu\tau$:

$$VB \quad : \quad \mathcal{B}\left(B \to K^{(*)}\mu\tau\right) \simeq 4.0 \times 10^{-10} \,,$$
$$U_1 \quad : \quad \mathcal{B}\left(B \to K^{(*)}\mu\tau\right)|_{\max} = 1.6 \times 10^{-7} \,. \tag{5.14}$$

When the coupling[2] is allowed to vary, the value of $\mathcal{B}(B \to K^{(*)}\mu\tau)|_{\max}$ predicted by the U_1 model is larger than in section 5.1. Unfortunately, it is still below the reach of Belle II (which is 5×10^{-7} [77]).

4. $B \to K^{(*)}\tau^+\tau^-$:

$$VB \quad : \quad \mathcal{B}\left(B \to K^{(*)}\tau^+\tau^-\right) \simeq 4.4 \times 10^{-8} \,,$$
$$U_1 \quad : \quad \mathcal{B}\left(B \to K^{(*)}\tau^+\tau^-\right)|_{\max} = 1.1 \times 10^{-4} \,. \tag{5.15}$$

Here too, when the coupling[2] is allowed to vary, we find that the value of $\mathcal{B}(B \to K^{(*)}\tau^+\tau^-)|_{\max}$ for the U_1 model is increased over that in section 5.1. It may just be attainable at Belle II (its reach is $\sim 2 \times 10^{-4}$ [77]). Thus, $B \to K^{(*)}\tau^+\tau^-$ could perhaps be used to distinguish the two models.

5. $B_s^0 \to \mu\tau$:

$$VB \quad : \quad \mathcal{B}\left(B_s^0 \to \mu\tau\right) \simeq 6.7 \times 10^{-9} \,,$$
$$U_1 \quad : \quad \mathcal{B}\left(B_s^0 \to \mu\tau\right)|_{\max} = 2.8 \times 10^{-6} \,. \tag{5.16}$$

Once again, the value of $\mathcal{B}(B_s^0 \to \mu\tau)|_{\max}$ for the U_1 model is larger than that in section 5.1. However, we cannot evaluate whether this decay can be used to distinguish the two models as we do not know the reach of LHCb or Belle II for $B_s^0 \to \mu\tau$.

6. $B_s^0 \to \tau^+\tau^-$

$$VB \quad : \quad \mathcal{B}\left(B_s^0 \to \tau^+\tau^-\right) \simeq 2.4 \times 10^{-7} \,,$$
$$U_1 \quad : \quad \mathcal{B}\left(B_s^0 \to \tau^+\tau^-\right)|_{\max} = 5.4 \times 10^{-4} \,. \tag{5.17}$$

The value of $\mathcal{B}(B_s^0 \to \tau^+\tau^-)|_{\max}$ for the U_1 model is larger than before. However, we cannot evaluate whether this decay can be used to distinguish the two models as we do not know the reach of LHCb or Belle II for $B_s^0 \to \tau^+\tau^-$.

7. $\Upsilon(3S) \to \mu\tau$:

$$VB \qquad \mathcal{B}(\Upsilon(3S) \to \mu\tau) \simeq 3.0 \times 10^{-9}\,,$$

$$U_1 \quad : \quad \mathcal{B}(\Upsilon(3S) \to \mu\tau)|_{\max} = 8.0 \times 10^{-7}\,. \tag{5.18}$$

Previously, we made a rough estimate that Belle II should be able to measure $\mathcal{B}(\Upsilon(3S) \to \mu\tau)$ down to $\sim 10^{-7}$. We speculated that perhaps Belle II could do better than this (and noted that a precise determination of the reach can only be obtained through a detailed study). However, the above predicted values of $\mathcal{B}(\Upsilon(3S) \to \mu\tau)|_{\max}$ show that, even with our rough estimate, the U_1 model can lead to rates for $\Upsilon(3S) \to \mu\tau$ that are easily observable at Belle II. If this decay were seen, it would exclude VB and point to U_1. This demonstrates the importance of this process for testing NP models in B decays.

5.3 Combining observables

Above, we have seen that it is indeed possible to distinguish the VB and U_1 models. VB predicts that $\tau \to 3\mu$ is on the verge of being observed, while there are several other observables that are signals of U_1. Should one of these signals be seen, indicating the presence of a particular type of NP, it would of course be very exciting. However, even more information about the underlying NP model can be obtained by using the measurements of other observables.

The U_1 model contains three unknown parameters: θ_L, θ_D and $|h_{U_1}^{33}|^2/\Lambda_{\rm NP}^2$. Then, given the measurement of an observable that indicates the presence of the U_1 model, one can use two other observables to derive the values of all the parameters of the model. To illustrate this, suppose that R_K and $R_{D^{(*)}}$ are measured very precisely, and $R_K = 0.781$ and $R_{D^{(*)}}^{\rm ratio} = 1.077$ are found. If $\mathcal{B}(\Upsilon(3S) \to \mu\tau) = 1.11 \times 10^{-8}$ is also measured, this points to the U_1 model. The theoretical parameters must take the values $|h_{U_1}^{33}|^2/\Lambda_{\rm NP}^2 = 2.43\,{\rm TeV}^{-2}$, $\theta_L = 0.039$, $\theta_D = 0.006$. U_1 then predicts $\mathcal{B}(B \to K^{(*)}\mu\tau) = 1.68 \times 10^{-8}$, $\mathcal{B}(B \to K^{(*)}\tau^+\tau^-) = 5.57 \times 10^{-6}$, $\mathcal{B}(B_s^0 \to \mu\tau) = 2.80 \times 10^{-7}$, and $\mathcal{B}(B_s^0 \to \tau^+\tau^-) = 2.57 \times 10^{-5}$.

On the other hand, the VB model is much more restrictive. It contains four unknown parameters: θ_L, θ_D, g_{qV}^{33} and g_{lV}^{33} (without loss of generality we can set $\Lambda_{\rm NP} = 1\,{\rm TeV}$). Unlike the U_1 model, the VB model receives severe constraints from B_s^0-$\bar{B}_s^0$ mixing and $\tau \to 3\mu$. The constraint from B_s^0-$\bar{B}_s^0$ mixing implies $g_{qV}^{33} \sin\theta_D \cos\theta_D < 4.2 \times 10^{-3}$, while the constraint from $\tau \to 3\mu$ implies $(g_{\ell V}^{33})^2 \sin^3\theta_L \cos\theta_L < 1.65 \times 10^{-2}$ at 90% C.L. These constraints leave no room for the VB model to explain R_K less than 0.90 at 90% or higher C.L.

6 Conclusions

At present, there are several measurements of B decays that exhibit discrepancies with the predictions of the SM. These include P_5' (from an angular analysis of $B \to K^*\mu^+\mu^-$), the differential branching fraction of $B_s^0 \to \phi\mu^+\mu^-$, $R_K \equiv \mathcal{B}(B^+ \to K^+\mu^+\mu^-)/\mathcal{B}(B^+ \to K^+e^+e^-)$, and $R_{D^{(*)}} \equiv \mathcal{B}(\bar{B} \to D^{(*)}\tau^-\bar{\nu}_\tau)/\mathcal{B}(\bar{B} \to D^{(*)}\ell^-\bar{\nu}_\ell)$ $(\ell = e, \mu)$. These suggest NP

in $\bar{b} \to \bar{s}\mu^+\mu^-$ (first three signals) or $\bar{b} \to \bar{c}\tau^+\nu_\tau$ ($R_{D^{(*)}}$). Now, suppose that NP is present, and that it couples preferentially to the left-handed third-generation particles in the gauge basis. In ref. [30], it was noted that, if this NP is invariant under the full $SU(3)_C \times SU(2)_L \times U(1)_Y$ gauge group, then, when one transforms to the mass basis, one generates the operators $(\bar{b}_L\gamma_\mu s_L)(\bar{\mu}_L\gamma^\mu\mu_L)$ (that contributes to $\bar{b} \to \bar{s}\mu^+\mu^-$) and $(\bar{b}_L\gamma_\mu c_L)(\bar{\tau}_L\gamma^\mu\nu_{\tau L})$ (that contributes to $\bar{b} \to \bar{c}\tau^+\nu_\tau$). In other words, the R_K and $R_{D^{(*)}}$ puzzles can be simultaneously explained.

This idea was explored in greater detail, using an effective field theory approach, in ref. [44]. Here the starting point is a model-independent effective Lagrangian consisting of two four-fermion operators in the gauge basis, each with its own coupling. It was assumed that the transformation from the gauge basis to the mass basis leads to mixing only between the second and third generations. As a consequence, for the down-type quarks, only one unknown theoretical parameter is introduced: θ_D. Similarly, for the charged leptons, θ_L is the new parameter. In the mass basis, the two operators contribute to a variety of B decays, all with two quarks and two leptons at the fermion level: $B \to K^*\mu^+\mu^-$, $B_s^0 \to \phi\mu^+\mu^-$, R_K, $R_{D^{(*)}}$, $B \to K^{(*)}\nu\bar{\nu}$. The coefficients of the operators in the mass basis are all functions of the coupling^2, θ_D and θ_L. For assumed values of the coupling^2, the experimental measurements lead to an allowed region in (θ_L, θ_D) space. This region was found to be nonzero, showing that a simultaneous explanation of R_K and $R_{D^{(*)}}$ is possible. There are two UV completions that can give rise to the effective Lagrangian. They are (i) VB: a vector boson that transforms as an $SU(2)_L$ triplet, as in the SM, and (ii) U_1: an $SU(2)_L$-singlet vector leptoquark.

The purpose of this paper is to explore ways of distinguishing the VB and U_1 models. There are two reasons to think that this might be possible. First, the VB model does not lead only to tree-level operators with two quarks and two leptons. It also produces four-quark and four-lepton operators. As such, it also contributes to processes such as B_s^0-$\bar{B}_s^0$ mixing and $\tau \to 3\mu$. These will lead to additional constraints on θ_D and θ_L, respectively. Second, while VB contributes to $B \to K^{(*)}\nu\bar{\nu}$, U_1 does not. The net effect is that the experimental constraints on the VB model are more stringent than those on the U_1 model. That is, the allowed region in (θ_L, θ_D) space is smaller for VB than for U_1. This implies that the predictions for the rates of other lepton-flavor-violating processes may be very different in the two models, which will allow us to distinguish them.

With this in mind, our first step was to apply the relevant experimental constraints to determine the allowed region in (θ_L, θ_D) space for each of the models. The constraints from the measurements of R_K, R_D, R_{D^*}, and $\tau \to \mu\phi$ applied to both models. For VB there were additional constraints from $B \to K^{(*)}\nu\bar{\nu}$, B_s^0-$\bar{B}_s^0$ mixing, and $\tau \to 3\mu$.

Our intention was to then use the allowed (θ_L, θ_D) regions to compute the predictions of the two models for various observables. However, the first step produced an unexpected result: the constraints on the VB model are so stringent that it is just barely viable. To be specific, the boundaries of the allowed (θ_L, θ_D) regions corresponding to the ΔM_s, $b \to s\mu\mu$, and $\tau \to 3\mu$ constraints overlap at essentially a single point. This is a very different result than that found in the effective field theory analysis of ref. [44]. This is because all constraints have been included in the present model-dependent analysis. This

illustrates that the results from the effective field theory analysis must be used carefully: despite being "model-independent," they do not necessarily apply to all models.

Things were very different for the U_1 model. We considered two possibilities for the coupling[2]: $\left|h_{U_1}^{33}\right|^2 = 1$ and $0.5 \leq \left|h_{U_1}^{33}\right|^2 \leq 5$. In either case, the allowed region in (θ_L, θ_D) space is sizeable.

For both models, using the allowed (θ_L, θ_D) regions, we then computed the predictions for various observables. Note that, since the (θ_L, θ_D) "region" of the VB model consists essentially of a single point, the predictions for the observables are very specific. On the other hand, the U_1 model gives ranges for its predictions. The observables include $R_{D^{(*)}}$, R_K, $\tau \to 3\mu$ (VB only), $B \to K^{(*)}\mu\tau$, $B \to K^{(*)}\tau^+\tau^-$, $B_s^0 \to \mu\tau$, $B_s^0 \to \tau^+\tau^-$ and $\Upsilon(3S) \to \mu\tau$. Note that the lepton-flavor-violating decay $\Upsilon(3S) \to \mu\tau$ has been overlooked in previous analyses. However, it is potentially an important process for testing models proposed to explain the B-decay anomalies.

Given that their allowed (θ_L, θ_D) regions are so different, it is indeed possible to distinguish the VB and U_1 models experimentally. VB predicts $\mathcal{B}(\tau^- \to \mu^-\mu^+\mu^-) \simeq 2.1 \times 10^{-8}$, which is the present upper limit. This is measurable at Belle II and LHCb, so that $\tau \to 3\mu$ constitutes a smoking-gun signal for the VB model. There is no similar observable for the U_1 model. However, there are a number of processes that can potentially point to U_1. We present the results for $0.5 \leq \left|h_{U_1}^{33}\right|^2 \leq 5$. For the decay $\Upsilon(3S) \to \mu\tau$, we estimated that Belle II should be able to measure its branching ratio down to $\sim 10^{-7}$. But the U_1 (VB) model predicts $\mathcal{B}(\Upsilon(3S) \to \mu\tau)|_{\max} = 8.0 \times 10^{-7}$ (3.0×10^{-9}). Thus, if this decay were observed, it would indicate U_1 (and exclude VB). Another possibility is R_K. Its present allowed 3σ range is $0.498 \leq R_K \leq 1.036$. The U_1 (VB) model predicts $0.51 \leq R_K \leq 0.90$ ($R_K \simeq 0.90$). The U_1 model can therefore accomodate smaller values of R_K than can the VB model, so that, if future measurements find $0.51 \leq R_K < 0.90$ at higher than 90% C.L., this would exclude VB and favor U_1. Finally, for the other decays $B \to K^{(*)}\mu\tau$, $B \to K^{(*)}\tau^+\tau^-$, $B_s^0 \to \mu\tau$, and $B_s^0 \to \tau^+\tau^-$, in all cases the U_1 model predicts larger branching ratios than does VB. However, whether or not these decays can be used to distinguish the two models depends on whether they can be observed at Belle II or LHCb.

Notes added. (1) While this paper was being completed, the Belle Collaboration released a new measurement of R_{D^*} [84]. They find consistency with the SM at the level of 0.6σ. Now, if this result is combined with the previous results of BaBar, Belle and LHCb, the discrepancy with the SM is reduced. However, in any case, neither of the VB and U_1 models presented in this paper allows for large deviations in $R_{D^{(*)}}$ from the SM. Thus, this result is rather favored. (2) After this paper was submitted to the arXiv, we were informed that LHCb has now set the upper limit $\mathcal{B}(B_s^0 \to \tau^+\tau^-) < 3.0 \times 10^{-3}$ (95% C.L.) [85].

Acknowledgments

References

[1] LHCb collaboration, *Measurement of Form-Factor-Independent Observables in the Decay $B^0 \to K^{*0}\mu^+\mu^-$*, *Phys. Rev. Lett.* **111** (2013) 191801 [arXiv:1308.1707] [INSPIRE].

[2] LHCb collaboration, *Angular analysis of the $B^0 \to K^{*0}\mu^+\mu^-$ decay using 3 fb^{-1} of integrated luminosity*, *JHEP* **02** (2016) 104 [arXiv:1512.04442] [INSPIRE].

[3] U. Egede, T. Hurth, J. Matias, M. Ramon and W. Reece, *New observables in the decay mode $\bar{B}_d \to \bar{K}^{*0}l^+l^-$*, *JHEP* **11** (2008) 032 [arXiv:0807.2589] [INSPIRE].

[4] BELLE collaboration, A. Abdesselam et al., *Angular analysis of $B^0 \to K^*(892)^0\ell^+\ell^-$*, arXiv:1604.04042 [INSPIRE].

[5] S. Descotes-Genon, T. Hurth, J. Matias and J. Virto, *Optimizing the basis of $B \to K^*ll$ observables in the full kinematic range*, *JHEP* **05** (2013) 137 [arXiv:1303.5794] [INSPIRE].

[6] S. Descotes-Genon, L. Hofer, J. Matias and J. Virto, *On the impact of power corrections in the prediction of $B \to K^*\mu^+\mu^-$ observables*, *JHEP* **12** (2014) 125 [arXiv:1407.8526] [INSPIRE].

[7] J. Lyon and R. Zwicky, *Resonances gone topsy turvy — the charm of QCD or new physics in $b \to s\ell^+\ell^-$?*, arXiv:1406.0566 [INSPIRE].

[8] S. Jäger and J. Martin Camalich, *Reassessing the discovery potential of the $B \to K^*\ell^+\ell^-$ decays in the large-recoil region: SM challenges and BSM opportunities*, *Phys. Rev.* **D 93** (2016) 014028 [arXiv:1412.3183] [INSPIRE].

[9] M. Ciuchini, M. Fedele, E. Franco, S. Mishima, A. Paul, L. Silvestrini et al., *$B \to K^*\ell^+\ell^-$ decays at large recoil in the Standard Model: a theoretical reappraisal*, *JHEP* **06** (2016) 116 [arXiv:1512.07157] [INSPIRE].

[10] S. Descotes-Genon, L. Hofer, J. Matias and J. Virto, *Global analysis of $b \to s\ell\ell$ anomalies*, *JHEP* **06** (2016) 092 [arXiv:1510.04239] [INSPIRE].

[11] T. Hurth, F. Mahmoudi and S. Neshatpour, *On the anomalies in the latest LHCb data*, *Nucl. Phys.* **B 909** (2016) 737 [arXiv:1603.00865] [INSPIRE].

[12] LHCb collaboration, *Differential branching fraction and angular analysis of the decay* $B_s^0 \to \phi\mu^+\mu^-$, *JHEP* **07** (2013) 084 [arXiv:1305.2168] [INSPIRE].

[13] LHCb collaboration, *Angular analysis and differential branching fraction of the decay* $B_s^0 \to \phi\mu^+\mu^-$, *JHEP* **09** (2015) 179 [arXiv:1506.08777] [INSPIRE].

[14] R.R. Horgan, Z. Liu, S. Meinel and M. Wingate, *Calculation of* $B^0 \to K^{*0}\mu^+\mu^-$ *and* $B_s^0 \to \phi\mu^+\mu^-$ *observables using form factors from lattice QCD*, *Phys. Rev. Lett.* **112** (2014) 212003 [arXiv:1310.3887] [INSPIRE].

[15] R.R. Horgan, Z. Liu, S. Meinel and M. Wingate, *Rare B decays using lattice QCD form factors*, PoS(LATTICE2014)372 [arXiv:1501.00367] [INSPIRE].

[16] A. Bharucha, D.M. Straub and R. Zwicky, $B \to V\ell^+\ell^-$ *in the Standard Model from light-cone sum rules*, *JHEP* **08** (2016) 098 [arXiv:1503.05534] [INSPIRE].

[17] LHCb collaboration, *Test of lepton universality using* $B^+ \to K^+\ell^+\ell^-$ *decays*, *Phys. Rev. Lett.* **113** (2014) 151601 [arXiv:1406.6482] [INSPIRE].

[18] M. Bordone, G. Isidori and A. Pattori, *On the Standard Model predictions for* R_K *and* R_{K^*}, *Eur. Phys. J.* **C 76** (2016) 440 [arXiv:1605.07633] [INSPIRE].

[19] BaBar collaboration, J.P. Lees et al., *Measurement of an Excess of* $\bar{B} \to D^{(*)}\tau^-\bar{\nu}_\tau$ *Decays and Implications for Charged Higgs Bosons*, *Phys. Rev.* **D 88** (2013) 072012 [arXiv:1303.0571] [INSPIRE].

[20] Belle collaboration, M. Huschle et al., *Measurement of the branching ratio of* $\bar{B} \to D^{(*)}\tau^-\bar{\nu}_\tau$ *relative to* $\bar{B} \to D^{(*)}\ell^-\bar{\nu}_\ell$ *decays with hadronic tagging at Belle*, *Phys. Rev.* **D 92** (2015) 072014 [arXiv:1507.03233] [INSPIRE].

[21] LHCb collaboration, *Measurement of the ratio of branching fractions* $\mathcal{B}(\bar{B}^0 \to D^{*+}\tau^-\bar{\nu}_\tau)/\mathcal{B}(\bar{B}^0 \to D^{*+}\mu^-\bar{\nu}_\mu)$, *Phys. Rev. Lett.* **115** (2015) 111803 [*Addendum ibid.* **115** (2015) 159901] [arXiv:1506.08614] [INSPIRE].

[22] B. Dumont, K. Nishiwaki and R. Watanabe, *LHC constraints and prospects for* S_1 *scalar leptoquark explaining the* $\bar{B} \to D^{(*)}\tau\bar{\nu}$ *anomaly*, *Phys. Rev.* **D 94** (2016) 034001 [arXiv:1603.05248] [INSPIRE].

[23] M. Tanaka and R. Watanabe, *New physics in the weak interaction of* $\bar{B} \to D^{(*)}\tau\bar{\nu}$, *Phys. Rev.* **D 87** (2013) 034028 [arXiv:1212.1878] [INSPIRE].

[24] A. Datta, M. Duraisamy and D. Ghosh, *Explaining the* $B \to K^*\mu^+\mu^-$ *data with scalar interactions*, *Phys. Rev.* **D 89** (2014) 071501 [arXiv:1310.1937] [INSPIRE].

[25] G. Hiller and M. Schmaltz, R_K *and future* $b \to s\ell\ell$ *physics beyond the standard model opportunities*, *Phys. Rev.* **D 90** (2014) 054014 [arXiv:1408.1627] [INSPIRE].

[26] D. Ghosh, M. Nardecchia and S.A. Renner, *Hint of Lepton Flavour Non-Universality in B Meson Decays*, *JHEP* **12** (2014) 131 [arXiv:1408.4097] [INSPIRE].

[27] T. Hurth, F. Mahmoudi and S. Neshatpour, *Global fits to* $b \to s\ell\ell$ *data and signs for lepton non-universality*, *JHEP* **12** (2014) 053 [arXiv:1410.4545] [INSPIRE].

[28] W. Altmannshofer and D.M. Straub, *New physics in* $b \to s$ *transitions after LHC run 1*, *Eur. Phys. J.* **C 75** (2015) 382 [arXiv:1411.3161] [INSPIRE].

[29] S.L. Glashow, D. Guadagnoli and K. Lane, *Lepton Flavor Violation in B Decays?*, *Phys. Rev. Lett.* **114** (2015) 091801 [arXiv:1411.0565] [INSPIRE].

[30] B. Bhattacharya, A. Datta, D. London and S. Shivashankara, *Simultaneous Explanation of the R_K and $R_{D^{(*)}}$ Puzzles*, *Phys. Lett.* **B 742** (2015) 370 [arXiv:1412.7164] [INSPIRE].

[31] A. Datta, M. Duraisamy and D. Ghosh, *Diagnosing New Physics in $b \to c\,\tau\,\nu_\tau$ decays in the light of the recent BaBar result*, *Phys. Rev.* **D 86** (2012) 034027 [arXiv:1206.3760] [INSPIRE].

[32] A. Celis, M. Jung, X.-Q. Li and A. Pich, *Sensitivity to charged scalars in $B \to D^{(*)}\tau\nu_\tau$ and $B \to \tau\nu_\tau$ decays*, *JHEP* **01** (2013) 054 [arXiv:1210.8443] [INSPIRE].

[33] A. Crivellin, A. Kokulu and C. Greub, *Flavor-phenomenology of two-Higgs-doublet models with generic Yukawa structure*, *Phys. Rev.* **D 87** (2013) 094031 [arXiv:1303.5877] [INSPIRE].

[34] I. Doršner, S. Fajfer, N. Košnik and I. Nišandžić, *Minimally flavored colored scalar in $\bar{B} \to D^{(*)}\tau\bar{\nu}$ and the mass matrices constraints*, *JHEP* **11** (2013) 084 [arXiv:1306.6493] [INSPIRE].

[35] M. Freytsis, Z. Ligeti and J.T. Ruderman, *Flavor models for $\bar{B} \to D^{(*)}\tau\bar{\nu}$*, *Phys. Rev.* **D 92** (2015) 054018 [arXiv:1506.08896] [INSPIRE].

[36] N.G. Deshpande and X.-G. He, *Consequences of R-Parity violating interactions for anomalies in $\bar{B} \to D^{(*)}\tau\bar{\nu}$ and $b \to s\mu^+\mu^-$*, arXiv:1608.04817 [INSPIRE].

[37] M.A. Ivanov, J.G. Körner and C.-T. Tran, *Analyzing new physics in the decays $\bar{B}^0 \to D^{(*)}\tau^-\bar{\nu}_\tau$ with form factors obtained from the covariant quark model*, *Phys. Rev.* **D 94** (2016) 094028 [arXiv:1607.02932] [INSPIRE].

[38] M. Duraisamy and A. Datta, *The Full $B \to D^*\tau^-\bar{\nu}_\tau$ Angular Distribution and CP-violating Triple Products*, *JHEP* **09** (2013) 059 [arXiv:1302.7031] [INSPIRE].

[39] M. Duraisamy, P. Sharma and A. Datta, *Azimuthal $B \to D^*\tau^-\bar{\nu}_\tau$ angular distribution with tensor operators*, *Phys. Rev.* **D 90** (2014) 074013 [arXiv:1405.3719] [INSPIRE].

[40] Y. Sakaki, M. Tanaka, A. Tayduganov and R. Watanabe, *Probing New Physics with q^2 distributions in $\bar{B} \to D^{(*)}\tau\bar{\nu}$*, *Phys. Rev.* **D 91** (2015) 114028 [arXiv:1412.3761] [INSPIRE].

[41] D. Das, C. Hati, G. Kumar and N. Mahajan, *Towards a unified explanation of $R_{D^{(*)}}$, R_K and $(g-2)_\mu$ anomalies in a left-right model with leptoquarks*, *Phys. Rev.* **D 94** (2016) 055034 [arXiv:1605.06313] [INSPIRE].

[42] C.-J. Lee and J. Tandean, *Minimal lepton flavor violation implications of the $b \to s$ anomalies*, *JHEP* **08** (2015) 123 [arXiv:1505.04692] [INSPIRE].

[43] D. Bečirević, S. Fajfer and N. Košnik, *Lepton flavor nonuniversality in $b \to sl^+l^-$ processes*, *Phys. Rev.* **D 92** (2015) 014016 [arXiv:1503.09024] [INSPIRE].

[44] L. Calibbi, A. Crivellin and T. Ota, *Effective field theory approach to $b \to s\ell\ell^{(\prime)}$, $B \to K^{(*)}\nu\bar{\nu}$ and $B \to D^{(*)}\tau\nu$ with third generation couplings*, *Phys. Rev. Lett.* **115** (2015) 181801 [arXiv:1506.02661] [INSPIRE].

[45] BaBar collaboration, J.P. Lees et al., *Search for $B \to K^{(*)}\nu\bar{\nu}$ and invisible quarkonium decays*, *Phys. Rev.* **D 87** (2013) 112005 [arXiv:1303.7465] [INSPIRE].

[46] Belle collaboration, O. Lutz et al., *Search for $B \to h^{(*)}\nu\bar{\nu}$ with the full Belle $\Upsilon(4S)$ data sample*, *Phys. Rev.* **D 87** (2013) 111103 [arXiv:1303.3719] [INSPIRE].

[47] R. Alonso, B. Grinstein and J. Martin Camalich, *Lepton universality violation and lepton flavor conservation in B-meson decays*, *JHEP* **10** (2015) 184 [arXiv:1505.05164] [INSPIRE].

[48] A. Crivellin, G. D'Ambrosio and J. Heeck, *Addressing the LHC flavor anomalies with horizontal gauge symmetries*, *Phys. Rev.* **D 91** (2015) 075006 [arXiv:1503.03477] [INSPIRE].

[49] A. Greljo, G. Isidori and D. Marzocca, *On the breaking of Lepton Flavor Universality in B decays*, *JHEP* **07** (2015) 142 [arXiv:1506.01705] [INSPIRE].

[50] D. Aristizabal Sierra, F. Staub and A. Vicente, *Shedding light on the $b \to s$ anomalies with a dark sector*, *Phys. Rev.* **D 92** (2015) 015001 [arXiv:1503.06077] [INSPIRE].

[51] C.-W. Chiang, X.-G. He and G. Valencia, *Z' model for $b \to s\ell\bar{\ell}$ flavor anomalies*, *Phys. Rev.* **D 93** (2016) 074003 [arXiv:1601.07328] [INSPIRE].

[52] S.M. Boucenna, A. Celis, J. Fuentes-Martin, A. Vicente and J. Virto, *Non-abelian gauge extensions for B-decay anomalies*, *Phys. Lett.* **B 760** (2016) 214 [arXiv:1604.03088] [INSPIRE].

[53] Y. Sakaki, M. Tanaka, A. Tayduganov and R. Watanabe, *Testing leptoquark models in $\bar{B} \to D^{(*)}\tau\bar{\nu}$*, *Phys. Rev.* **D 88** (2013) 094012 [arXiv:1309.0301] [INSPIRE].

[54] B. Gripaios, M. Nardecchia and S.A. Renner, *Composite leptoquarks and anomalies in B-meson decays*, *JHEP* **05** (2015) 006 [arXiv:1412.1791] [INSPIRE].

[55] I. de Medeiros Varzielas and G. Hiller, *Clues for flavor from rare lepton and quark decays*, *JHEP* **06** (2015) 072 [arXiv:1503.01084] [INSPIRE].

[56] R. Barbieri, G. Isidori, A. Pattori and F. Senia, *Anomalies in B-decays and $U(2)$ flavour symmetry*, *Eur. Phys. J.* **C 76** (2016) 67 [arXiv:1512.01560] [INSPIRE].

[57] S. Fajfer and N. Košnik, *Vector leptoquark resolution of R_K and $R_{D^{(*)}}$ puzzles*, *Phys. Lett.* **B 755** (2016) 270 [arXiv:1511.06024] [INSPIRE].

[58] S. Sahoo, R. Mohanta and A.K. Giri, *Explaining R_K and $R_{D^{(*)}}$ anomalies with vector leptoquark*, arXiv:1609.04367 [INSPIRE].

[59] A.J. Buras, J. Girrbach-Noe, C. Niehoff and D.M. Straub, *$B \to K^{(*)}\nu\bar{\nu}$ decays in the Standard Model and beyond*, *JHEP* **02** (2015) 184 [arXiv:1409.4557] [INSPIRE].

[60] ALEPH collaboration, R. Barate et al., *Measurements of $BR(b \to \tau^-\bar{\nu}_\tau X)$ and $BR(b \to \tau^-\bar{\nu}_\tau D^{*\pm}X)$ and upper limits on $BR(B^- \to \tau^-\bar{\nu}_\tau)$ and $BR(b \to s\bar{\nu})$*, *Eur. Phys. J.* **C 19** (2001) 213 [hep-ex/0010022] [INSPIRE].

[61] PARTICLE DATA GROUP collaboration, K.A. Olive et al., *Review of Particle Physics*, *Chin. Phys.* **C 38** (2014) 090001 [INSPIRE].

[62] A. Datta, X.G. He and S. Pakvasa, *Quasiinclusive and exclusive decays of B to eta-prime*, *Phys. Lett.* **B 419** (1998) 369 [hep-ph/9707259] [INSPIRE].

[63] B. Bhattacharya and J.L. Rosner, *Effect of η-η' mixing on $D \to PV$ decays*, *Phys. Rev.* **D 82** (2010) 037502 [arXiv:1005.2159] [INSPIRE].

[64] BELLE collaboration, Y. Miyazaki et al., *Search for Lepton-Flavor-Violating tau Decays into a Lepton and a Vector Meson*, *Phys. Lett.* **B 699** (2011) 251 [arXiv:1101.0755] [INSPIRE].

[65] G. Buchalla, A.J. Buras and M.E. Lautenbacher, *Weak decays beyond leading logarithms*, *Rev. Mod. Phys.* **68** (1996) 1125 [hep-ph/9512380] [INSPIRE].

[66] S. Aoki et al., *Review of lattice results concerning low-energy particle physics*, *Eur. Phys. J.* **C 74** (2014) 2890 [arXiv:1310.8555] [INSPIRE].

[67] S. Aoki et al., *Review of lattice results concerning low-energy particle physics*, arXiv:1607.00299 [INSPIRE].

[68] J. Charles et al., *Current status of the Standard Model CKM fit and constraints on $\Delta F = 2$ New Physics*, *Phys. Rev.* **D 91** (2015) 073007 [arXiv:1501.05013] [INSPIRE].

[69] K.G. Chetyrkin, J.H. Kuhn and M. Steinhauser, *RunDec: A Mathematica package for running and decoupling of the strong coupling and quark masses*, *Comput. Phys. Commun.* **133** (2000) 43 [hep-ph/0004189] [INSPIRE].

[70] HEAVY FLAVOR AVERAGING GROUP (HFAG) collaboration, Y. Amhis et al., *Averages of b-hadron, c-hadron and τ-lepton properties as of summer 2014*, arXiv:1412.7515 [INSPIRE].

[71] K. Hayasaka et al., *Search for Lepton Flavor Violating Tau Decays into Three Leptons with 719 Million Produced Tau+Tau- Pairs*, *Phys. Lett.* **B 687** (2010) 139 [arXiv:1001.3221] [INSPIRE].

[72] F. Feruglio, P. Paradisi and A. Pattori, *Revisiting Lepton Flavour Universality in B Decays*, arXiv:1606.00524 [INSPIRE].

[73] David Straub, *flavio v0.11, 2016*, http://dx.doi.org/10.5281/zenodo.59840.

[74] J.-G. Shiu (National Taiwan University) on behalf of the Belle II collaboration, *BelleII: physics and early measurements*, talk given at *Beauty 2016*, Marseille, France, https://indico.cern.ch/event/352928/contributions/1757317.

[75] LHCb collaboration, *Letter of Intent for the LHCb Upgrade*, CERN-LHCC-2011-001.

[76] BABAR collaboration, B. Aubert et al., *Search for the decay $B^+ \to K^+\tau^\mp\mu^\pm$*, *Phys. Rev. Lett.* **99** (2007) 201801 [arXiv:0708.1303] [INSPIRE].

[77] S. Robertson and P. Urquijo, private communication.

[78] BABAR collaboration, J.P. Lees et al., *Search for $B^+ \to K^+\tau^+\tau^-$ at the BaBar experiment*, arXiv:1605.09637 [INSPIRE].

[79] T. Gershon, F. Polci and J. Serrano, private communication.

[80] A. Datta, P.J. O'Donnell, S. Pakvasa and X. Zhang, *Flavor changing processes in quarkonium decays*, *Phys. Rev.* **D 60** (1999) 014011 [hep-ph/9812325] [INSPIRE].

[81] BABAR collaboration, J.P. Lees et al., *Search for Charged Lepton Flavor Violation in Narrow Upsilon Decays*, *Phys. Rev. Lett.* **104** (2010) 151802 [arXiv:1001.1883] [INSPIRE].

[82] CLEO collaboration, W. Love et al., *Search for Lepton Flavor Violation in Upsilon Decays*, *Phys. Rev. Lett.* **101** (2008) 201601 [arXiv:0807.2695] [INSPIRE].

[83] D.A. Faroughy, A. Greljo and J.F. Kamenik, *Confronting lepton flavor universality violation in B decays with high-p_T tau lepton searches at LHC*, *Phys. Lett.* **B 764** (2017) 126 [arXiv:1609.07138] [INSPIRE].

[84] A. Abdesselam et al., *Measurement of the τ lepton polarization in the decay $\bar{B} \to D^*\tau^-\bar{\nu}_\tau$*, arXiv:1608.06391 [INSPIRE].

[85] K. De Bruyn (LHCb Collaboration), *Tests of Lepton Universality at LHCb*, talk at TAU2016, LHCb-CONF-2016-011, http://indico.ihep.ac.cn/event/5221/session/12/contribution/69/material/slides/0.pdf.